Self-consistent description of heavy nuclei. II. Spectroscopic properties of some odd nuclei

J. Libert
Centre de Spectroscopie Nucléaire et de Spectrométrie de Masse, Bâtiment 104, Campus Orsay, 91406 Orsay, France

M. Meyer
Institut de Physique Nucléaire (et IN2P3), Université Lyon I, 69622 Villeurbanne-Cedex, France

P. Quentin
Institut Laue-Langevin, 156X, 38042 Grenoble-Cedex, France
(Received 30 June 1981)

Spectroscopic properties of 23 odd nuclei within and around the actinide region have been calculated according to a rotor plus quasiparticle approximation where the quasiparticle states have been extracted from self-consistent calculations discussed in a previous paper. The phenomenological parameters are only six force parameters fitted once for all to nuclear saturation properties, neutron and proton pairing gaps uniquely given by odd-even mass differences, and experimental ground band energies of neighboring nuclei. Excluding thus any elusive *ad hoc* parameter adjustment, this approach has successfully reproduced most of the experimentally confirmed rotational bands for both odd-neutron (thorium, uranium, and plutonium) and odd-proton (actinium, protactinium, neptunium, and americium) isotopes, assessing thus the validity of the whole approach and, in particular, the relevance of the self-consistent deformed mean fields yielded by the Skyrme *S*III effective force. Many bands previously assigned to be of a particle-vibration nature have not been found in our calculations. Their nonrotational character is thus confirmed. Reduced transition probabilities and static moments for $E2$ and $M1$ electromagnetic modes have been evaluated. Calculated magnetic and electric quadrupole moments have been shown to reproduce very well available data. Absolute intraband and interband $E2$ and $M1$ reduced transition probabilities have also been found in very good agreement with experimental results.

[NUCLEAR STRUCTURE 23 heavy odd nuclei from ^{229}Th, ^{229}Ac to ^{241}Am, ^{241}Pu studied within rotor plus quasiparticle approximation. Quasiparticle states issued from Hartree-Fock plus BCS calculations using Skyrme *S*III force. Nuclear spectra, $E2$ and $M1$ moments and transition probabilities calculated.]

I. INTRODUCTION

In an accompanying paper[1] (hereafter referred to as I) the results of self-consistent calculations of very heavy nuclei have been discussed. These calculations have been performed within the Hartree-Fock (HF) plus Bardeen-Cooper-Shrieffer (BCS) approximation, using the Skyrme *S*III phenomenological effective force.[2] In the present paper we would like to assess the validity of the HF mean fields which have been obtained in I. For this purpose we will compare theoretical and experimental spectroscopic data for odd nuclei assuming that the latter are adequately described within the rotor plus one-quasiparticle (qp) approximation,[3] where the qp states are those stemming from our self-consistent calculations. The model Hamiltonian as well as the method for diagonalizing it, has been described previously[4] and discussed in the case of transitional cadmium isotropes. Even though the results of Ref. 4 were found in satisfactory agreement with experimental data, it was *a priori* noticed that the whole approach might suffer from the questionable adequacy of the rotor approximation for such soft nuclei. It is, therefore, particularly interesting to investigate the accuracy of such a model description in a situation where its basic assumption is maximally fulfilled. This is why we have undertaken an extensive study of odd actinium, thorium, protactinium, uranium, neptunium, plutonium, and americium isotopes as specified on Fig. 1. From eight even cores calculated in I, we have computed the spectroscopic properties of 23 odd nuclei. We have also evaluated (in addition to what was done for cadmium isotopes in Ref. 4), $M1$ and $E2$ static moments and reduced transition probabilities. These quantities provide indeed stringent tests of the detailed structure of the single particle (sp) states obtained in our HF plus BCS calculations.

This paper will be organized as follows. Section II will be devoted to a brief survey of some calculational details in which after pointing out the physical assumptions pertaining to our approach, we will shortly describe the computation of moments and transition probabilities. The results which have been obtained will be discussed in Secs. III and IV for both odd N and odd Z isotopes. Finally, some conclusions will be drawn in Sec. V.

II. GENERAL SURVEY OF OUR CALCULATIONS

A. The model Hamiltonian

In the framework of the rotor plus qp model, the total Hamiltonian of an odd-A nucleus is given by:

$$H = H_{\text{int}} + H_{\text{rot}} , \tag{1}$$

where H_{int} is an independent qp Hamiltonian which is defined in terms of the HF plus BCS solutions obtained for all the considered even nuclei in their equilibrium deformation shape in I, to which we refer for further details.

Assuming an axially symmetric core rotating about an axis perpendicular to the symmetry axis ($R_z = 0$ with usual notation) the collective kinetic energy term H_{rot} can be written as:

$$H_{\text{rot}} = \frac{\hbar^2}{2\mathcal{I}}\vec{\mathrm{R}}^2 = \frac{\hbar^2}{2\mathcal{I}}(\vec{\mathrm{I}}^2 - 2I_z j_z) + \frac{\hbar^2}{2\mathcal{I}}\vec{\mathrm{j}}^2 - \frac{\hbar^2}{2\mathcal{I}}(j_- I_+ + j_+ I_-) , \tag{2}$$

where $\mathcal{I}$ is the moment of inertia and $\vec{\mathrm{R}}$, $\vec{\mathrm{I}}$, and $\vec{\mathrm{j}}$ are the core, total, and qp angular momenta. In order to introduce a variable moment of inertia in H_{rot} (i.e., such that $\mathcal{I}$ depends on R) has been suggested[5] to project the $|\alpha IMK\rangle$ basis states onto eigenstates $|\beta IMjR\rangle$ of the core and qp angular momenta (to which we will refer from now on as core basis states). In this case, the matrix elements of H can be written:

$$\langle \alpha IMK | H | \alpha' IMK' \rangle = \delta_{KK'}\delta_{\alpha\alpha'}\mathcal{E}_{\alpha K} + \sum_{\beta\beta' R} A^I_{\beta jR,\alpha K} A^I_{\beta' jR,\alpha' K'} \frac{\hbar^2}{2\mathcal{I}(R)} R(R+1)(u_{\alpha K}u_{\alpha' K'} + v_{\alpha K}v_{\alpha' K'}) , \tag{3}$$

where $\mathcal{E}_{\alpha K}$, $u_{\alpha K}$, $v_{\alpha K}$ are the qp energy and pairing occupation factors of the considered (α,K) state, and where the A factors are simply expansion coefficients of the standard unified basis states on core basis states;

$$A^I_{\beta jR,\alpha K} = \langle \beta IMjR | \alpha IMK \rangle = \sqrt{2}\delta_{R,\text{even}} \langle \beta jK | \alpha K \rangle \left[\frac{2R+1}{2I+1}\right]^{1/2} \langle jKR\,0 | IK \rangle . \tag{4}$$

In Eq. (4) the last term is a Clebsch-Gordan coefficient and all the structural information on the qp wave function is concentrated into the overlap factor $\langle \beta jK | \alpha K \rangle$, whose numerical evaluation has been discussed in Ref. 4. A definite advantage of the consideration of such an H_{rot} term lies in the fact that its eigenvalues are simply the experimental ground state (g.s.) band energies. The introduction in Eq. (3) of the pairing factor has been discussed in Ref. 6.

After having diagonalized the energy matrix defined by Eq. (3) we obtain approximate odd-A nuclear states which will be noted in what follows as

$$|\gamma IM\rangle = \sum_{\alpha K} C^{\gamma}_{\alpha K} |\alpha IMK\rangle . \tag{5}$$

We have retained in the actual calculations all $|\alpha IMK\rangle$ states corresponding to qp states whose HF energies were lying in a band of 4 MeV above and 4 MeV below the Fermi level. As a typical example, this has led in ^{236}U+1 qp calculations, to the inclusion of 24 neutron and 18 proton qp states in the diagonalization subspace. In fact the practical size of the energy matrix turned out to be reduced—roughly by a factor of 2—due to the conservation of the parity symmetry.

B. Discussion of the model assumptions

First of all, it should be emphasized that our approach is consistent with a pure rotational core assumption. The explicit coupling term between the core and qp degrees of freedom is directly related to the assumption of a rotorlike kinetic collective energy as demonstrated in Eq. (2). As a consequence of the latter we will be able to give some support to previous assignments of bands as qp-vibration coupling bands by not finding them in our calculational results.

Merging experimental core g.s. band energies with calculated qp energies could be thought of as a somewhat inconsistent procedure. As a matter of fact, this is most probably not so inconsistent. Indeed as shown in I, a very good reproduction of relevant core static nuclear properties (including deformation properties) has been obtained with the effective force in use. Moreover, as seen in Table I, the moments of inertia calculated with the Inglis cranking formula from our self-consistent solutions[7] are in reasonable agreement with experimental data. Indeed, as it was the case for other modes,[8] the absence of Thouless-Valatin self-consistency contributions might account for the systematically too low (by $\sim 25-30\,\%$) values of calculated moments of inertia with respect to experimental ones.

TABLE I. Comparison between experimental and Inglis cranking values of the moment of inertia $\mathscr{I}$ for the ^{230}Th and ^{236}U nuclei. The listed rotational parameters $\mathscr{A}$ are equal to $2\mathscr{I}/h^2$ and expressed in MeV^{-1}. The experimental value is equal to $6/E_{2^+}$, where E_{2^+} is the experimental first 2^+ excitation energy. The cranking collective gyromagnetic ratio $g_R^{\rm cr}$ and its rough approximation Z/A are also given. These results have been extracted from Ref. 7.

Nucleus	$\mathscr{A}_{\rm cr}$	$\mathscr{A}_{\rm exp}$	$g_R^{\rm cr}$	Z/A
^{230}Th	78	113	0.245	0.391
^{236}U	102	132	0.250	0.390

For the sake of numerical feasibility, we have imposed axial symmetry to our solutions. Whereas this restriction may potentially constitute a definite drawback in transitional nuclei (this is not always so though, see, e.g., the case of light cadmium[4] or silver[9] isotopes), it is a fairly reasonable assumption for the well deformed actinide nuclei.

The parameters of our approach either have been fitted in a completely different context or are defined without any ambiguity, given the basic assumptions of the model. These parameters are six effective force parameters, the proton and the neutron pairing gaps, and the values $\mathscr{I}(R)$ of the core variable moment of inertia. Neither the pairing gaps nor the moment of inertia values are subject to any arbitrarily free choice since they are uniquely determined by odd-even binding energy differences for the former, and by g.s. band energies of the neighboring even nuclei for the latter. The force parameters have been fitted once for all,[2] with respect to nuclear matter saturation properties or equivalently with respect to binding energies and charge radii of few magic nuclei, and of course they have not been changed. It should also be noted that we have also not enjoyed any freedom in fixing arbitrarily the mean field deformation since our qp states have been computed from the equilibrium HF plus BCS solutions. In other words, apart from an *a priori* choice of the self-consistent symmetries (axial and parity symmetries) we have been left with no choice at all for the β_2, β_4, . . . values entering the calculations.

One should also mention that we have included the full $H_{\rm rot}$ term in our calculations. We have therefore included the so-called one-body recoil term $\vec{j}^{\,2}$. In the same way we have taken into account the exact Coriolis term which can be reformulated by saying that we have *not* used any attenuation factor.

An important feature of our calculations lies in the microscopic nature of the sp wave function determination. Among other characteristic properties, it has often been noted (see, e.g., Table I in Ref. 10) that they strongly mix basis states belonging to different major shells (indeed significantly more than in both modified harmonic oscillator or Woods-Saxon wells). Incidentally, it may be noticed that so-called $\Delta N=2$ couplings are included in a natural way in our self-consistent sp states. In any case, it is interesting to notice the relative richness in small basis state components. Whereas for some quantities like energies or some intraband electromagnetic transitions, etc., one does not need more than a rough sketch of the sp wave functions, there are indeed some spectroscopic quantities which require a far more detailed description. As an example of the latter, we refer to the particular case of $h\,\frac{11}{2}$ neutron band states in ^{107}Cd studied in Ref. 4: While the yrast state energy sequence was found to be characteristic of a decoupled band, the corresponding wave functions were indeed very poorly represented as pure decoupled states (e.g., only 61% of $j=\frac{11}{2}$, $R=0$ components for the $\frac{11}{2}^-$ band head state). It should be noted, however, that a correct reproduction of some interband transitions, for instance, is not only contingent upon the qp wave function structure but also upon the Coriolis mixing rate. Since we do not enjoy the freedom of adjustable qp energies, as in purely phenomenological approaches, it may happen for a given spin that a small error in the difference between two such energies will result in a sizable band mixing which would not be present otherwise.

Finally, one may raise questions about the motivation for undertaking a seemingly unequal composition of sophisticated HF plus BCS calculations with the rather crude rotor plus qp approximation. Indeed, how crude the latter approximation is constitutes precisely the question we would like to answer. However, in order not to completely blur the issue, we have found it necessary to insert the best available qp states as well as to avoid any phenomenological readjustment that would not be under theoretical control.

C. $E2$ and $M1$ reduced transition probabilities and moments

The basic formulas and general methods to evaluate $E2$ and $M1$ spectroscopic properties of the calculated eigenstates of H will be recalled in Appendix A. Appendix B presents some details concerning their numerical evaluation.

The neutron effective charge of the intrinsic $E2$ operator is taken equal to the proton charge. In most cases the contribution of the intrinsic $E2$ operator to either the quadrupole moment or the $B(E2)$ value will be negligible as compared to the contribution of the core operator. This is of course so only for intraband transitions or interband transitions between nuclear states having a sizable intrinsic state overlap.

For the evaluation of $M1$ properties we have taken the following gyromagnetic ratios:

$$g_l=0,1 \text{ for } n,p, \text{ respectively }, \tag{6}$$

$$g_s=-3.82,5.58 \text{ for } n,p, \text{ respectively }. \tag{7}$$

It is well known (see, e.g., Ref. 11) that both configuration mixing and meson exchange currents lead to a renormalization of sp gyromagnetic factors g_l and g_s. In order to roughly sketch the possible influence of such renormalizations, we will present below two sets of calculations of $M1$ properties, one using free g_s values and another using g_s values decreased by 40% (in all cases the free g_l values have been kept).

As for the core gyromagnetic ratio g_R, one obtains[7,12,13] in the cranking model approximation

$$g_R=\frac{\mathscr{I}^p_{\rm cr}}{\mathscr{I}_{\rm cr}}+(g_s^p-1)\frac{W^p}{\mathscr{I}_{\rm cr}}+g_s^n\frac{W^n}{\mathscr{I}_{\rm cr}}\ , \tag{8}$$

where the superscripts p and n refer to neutron and proton distributions and the nonsuperscribed quantities correspond to the total nucleonic distribution. In Eq. (8) the quantity W^p (and similarly W^n) is defined by:

$$W_p=\sum_{\mu\nu}\frac{(u_\mu v_\nu-u_\nu v_\mu)^2}{\mathscr{E}_\mu+\mathscr{E}_\nu}[\langle\mu\,|\,s_-\,|\,\nu\rangle\langle\nu\,|\,j_+\,|\,\mu\rangle+\tfrac{1}{2}\delta_{K\mu,1/2}\delta_{K\nu,1/2}\langle\bar\mu\,|\,s_-\,|\,\nu\rangle\langle\nu\,|\,j_+\,|\,\bar\mu\rangle]\ , \tag{9}$$

where the sums run over proton sp states having a positive third component K of the total angular momentum ($\mathscr{E}$, u, v being the corresponding qp energies and pairing occupation factors). Now it turns out that with the considered values [see Eq. (7)] of g_s^p and g_s^n the last two terms in Eq. (8) almost cancel each other, and, therefore, upon assuming the ratio of charge and matter moments of inertia to be approximated by the ratio of the norm of the two corresponding densities, one usually infers that

$$g_R \simeq Z/A \ . \tag{10}$$

In Ref. 7 the validity of the approximation (10) to g_R has been numerically checked for many nuclei and we reproduce in Table I the results obtained there for two actinide nuclei. In the present calculations we have consistently used the approximate Z/A value for g_R. However, we will discuss in Sec. IV the practical influence of such a choice on calculated $M1$ properties.

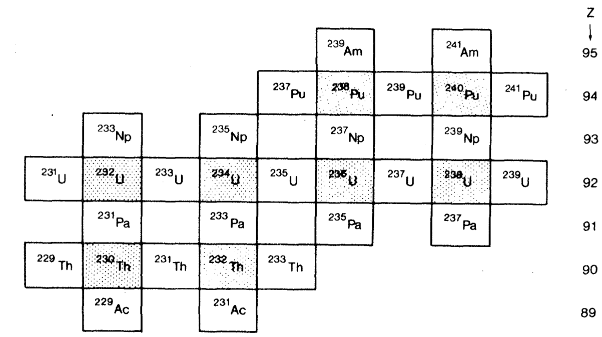

FIG. 1. Odd heavy nuclei studied in the present work. In grey boxes we have figured the even-even cores whose self-consistent solutions have been extracted from the HF plus BCS calculations of I.

III. EXCITATION ENERGY SPECTRA

Out of the HF plus BCS results of I concerning 15 even nuclei, we have selected those concerning eight even thorium, uranium, and plutonium isotopes (see Fig. 1). From these we have had access within our rotor plus qp approach to 11 odd-neutron isotopes and to 12 odd-proton (i.e., actinium, protactinium, neptunium, and americium) isotopes. Nine out of these 23 odd isotopes have been reached from both neighboring even-even cores allowing us thus to estimate the uncertainties associated with the rather crude one-quasiparticle character of our intrinsic wave functions.

We will start the presentation of our results by a discussion of excitation energy spectra.[14] On Fig. 2, we compare the variation with A of experimental[15–23] and calculated band heads for the studied uranium isotopes. Only experimental data

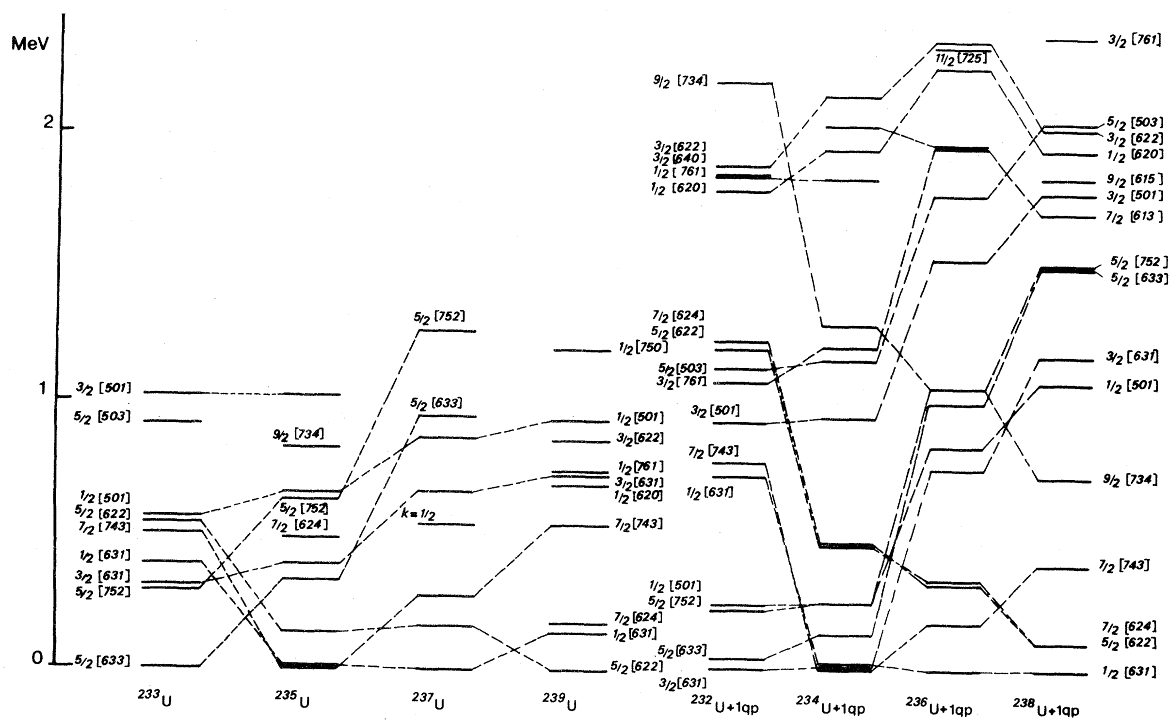

FIG. 2. Comparison of experimental energy band heads in ^{233,235,237,239}U with those calculated in terms of one neutron quasiparticle coupled to ^{232,234,236,238}U cores.

corresponding to a confirmed rotational band structure have been considered. As for the theoretical results, the band character has been ascertained by the weak Coriolis mixing of $|\alpha IMK\rangle$ basis states resulting from our diagonalization (for this matter and a discussion of the usual asymptotic quantum number assignment see the discussion of Table II below). For the five bands ($\frac{3}{2}^+[631]$, $\frac{1}{2}^+[631]$, $\frac{7}{2}^-[743]$, $\frac{5}{2}^+[622]$, and $\frac{1}{2}^-[501]$) whose evolution is well known from ^{233}U to ^{239}U, our calculations yield an excellent agreement with the observed trends. In particular, the energy difference between the $\frac{7}{2}^-[743]$ and $\frac{1}{2}^+[631]$ band heads which has proven in previous theoretical works[24] to be very difficult to reproduce, is in the present work well estimated.

On Fig. 3, we reproduce the theoretical evolution of band heads for some thorium and plutonium isotopes. These results are found strikingly similar to what was found (see Fig. 2) for the same neutron number in the uranium isotopes. As a particularly clear example, one may single out the level sequence in ^{238}Pu, ^{240}Pu$+1$ qp compared with the level sequence in ^{236}U, ^{238}U$+1$ qp. The four bands

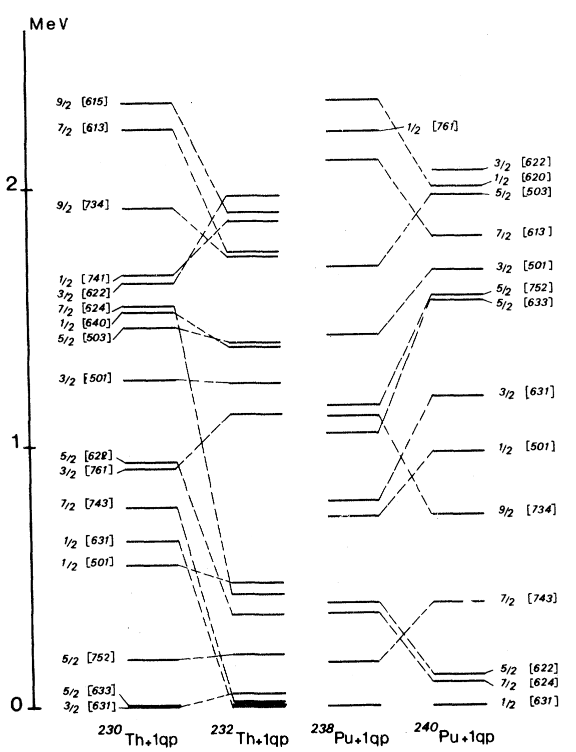

FIG. 3. Theoretical energy band heads in ^{229,231,233}Th and ^{237,239,241}Pu calculated in terms of one neutron quasiparticle coupled to ^{230,232}Th and ^{238,240}Pu cores.

experimentally known in ^{237,239,241}Pu isotopes[15–17] are correctly reproduced in our calculations. A more detailed discussion of the ^{231}Th and ^{233}Th isotopes will be found below.

Turning now to odd-proton isotopes, we present on Fig. 4 a comparison between experimental band heads in ^{233,235,237,239}Np (Refs. 15–17 and 25) and the results of our calculations using both uranium and plutonium even cores. There are indeed some uncertainties left in the experimental assignment of some band heads, particularly for the lighter neptunium isotopes. In this case, however, the agreement between the calculated evolution and what is experimentally known is excellent with the exception of the $\frac{5}{2}^+[642]$ band heads calculated from uranium cores at a slightly too high energy, and whose energies relative to the $\frac{5}{2}^-[523]$ are not found as constant as they should. For the heaviest isotopes, where a full comparison is possible, the spectra obtained with plutonium cores reproduce better experimental data than what has been obtained with uranium cores.

A comparison of results concerning proton qp states coupled to ^{230}Th and ^{232}Th cores with ^{231}Pa (Ref. 15) and ^{233}Pa (Refs. 16, 26) experimental data [to the best of our knowledge, no band assignment is available in ^{239}Ac (Ref. 16) and ^{231}Pa (Ref. 15)] is shown on Fig. 5. Apart from the $\frac{5}{2}^+[642]$ band head which is calculated as noted above at too high an energy, we fairly well reproduce known low energy data. We confirm, in particular, the assignment of $\frac{1}{2}^+[400]$ and $\frac{3}{2}^-[521]$ band heads.

For some selected isotopes we will now make a detailed comparison of the full experimental spectra with our calculated results. We will start with a study of ^{231}Th data[15,23,27] compared on Fig. 6 with theoretical energies obtained in calculations using both adjacent even cores. The six lowest bands are reproduced within a few 100 keV. Three bands ($\frac{1}{2}^-[501]$, $\frac{3}{2}^-[761]$, and $\frac{3}{2}^-[501]$) whose "experimental" assignments were only tentative have been confirmed. The $\frac{5}{2}^-[503]$ band proposed recently at an excitation energy of ~ 0.7 MeV is found, but at a rather high energy (~ 1.4 MeV with the ^{232}Th core). The so-called "$\frac{1}{2}^+[640]$" band for which only the sequence $\frac{7}{2}^+$, $\frac{5}{2}^+$, and $\frac{11}{2}^+$ has been proposed from (d,t) experiments,[28] would correspond, if its assignment were true, to a decoupling parameter $a \simeq -2$. However, we have not found in the right range of energy (i.e., around 650 keV) any such $\frac{1}{2}^+$ band, but rather a band resulting from the coupling of the $\frac{7}{2}^+[624]$ and $\frac{5}{2}^+[622]$ qp states (see the mixing coefficients in

TABLE II. Main components of band head ^{231}Th wave functions calculated as $^{230}Th+1$ qp and $^{232}Th+1$ qp states. The usual "experimental" assignment is given and compared with our theoretical results. For each qp state we have reported the percentage of main asymptotic basis components. For each band head state we have also given the major Coriolis mixed qp components.

Usual assignment	$^{230}Th+1$ qp calculations	$^{232}Th+1$ qp calculations
$\frac{5}{2}^+[633]$	91% $\frac{5}{2}\{50\%[633]\}$	97% $\frac{5}{2}\{54\%[633]\}$
$\frac{1}{2}^+[631]$	100% $\frac{1}{2}\{23\%[631]+11\%[611]+8\%[431]+7\%[851]\}$	100% $\frac{1}{2}\{25\%[631]+10\%[611]+9\%[431]+7\%[851]\}$
$\frac{3}{2}^+[631]$	99% $\frac{3}{2}\{26\%[631]+12\%[611]+10\%[431]+8\%[851]\}$	69% $\frac{3}{2}\{28\%[631]+11\%[431]+10\%[611]\}$ + 31% $\frac{1}{2}\{25\%[631]+10\%[611]+9\%[431]+7\%[851]\}$
$\frac{5}{2}^-[752]$	98% $\frac{5}{2}\{25\%[532]+24\%[752]\}$	99% $\frac{5}{2}\{30\%[752]+24\%[732]\}$
$\frac{5}{2}^+[622]$	99% $\frac{5}{2}\{32\%[622]+13\%[422]+10\%[822]\}$	97% $\frac{5}{2}\{34\%[622]+13\%[422]+11\%[822]\}$
$\frac{7}{2}^-[743]$	94% $\frac{7}{2}\{42\%[743]+18\%[723]\}$	79% $\frac{7}{2}\{47\%[743]+17\%[723]\}$ + 20% $\frac{5}{2}\{30\%[752]+24\%[732]\}$
$\frac{1}{2}^-[501]$	100% $\frac{1}{2}\{29\%[701]+24\%[501]\}$	100% $\frac{1}{2}\{30\%[701]+25\%[501]\}$
$\frac{3}{2}^-[761]$	97% $\frac{3}{2}\{25\%[741]+15\%[981]+10\%[761]\}$	86% $\frac{3}{2}\{25\%[741]+15\%[761]+14\%[981]\}$
$\frac{3}{2}^-[501]$	99% $\frac{3}{2}\{30\%[701]+24\%[301]+24\%[501]\}$	88% $\frac{3}{2}\{31\%[701]+24\%[301]+24\%[501]\}$
"$\frac{1}{2}^+[640]$"	90% $\frac{7}{2}\{62\%[624]\}$	78% $\frac{7}{2}\{64\%[624]\}$ + 18% $\frac{5}{2}\{34\%[622]+13\%[422]+11\%[822]\}$

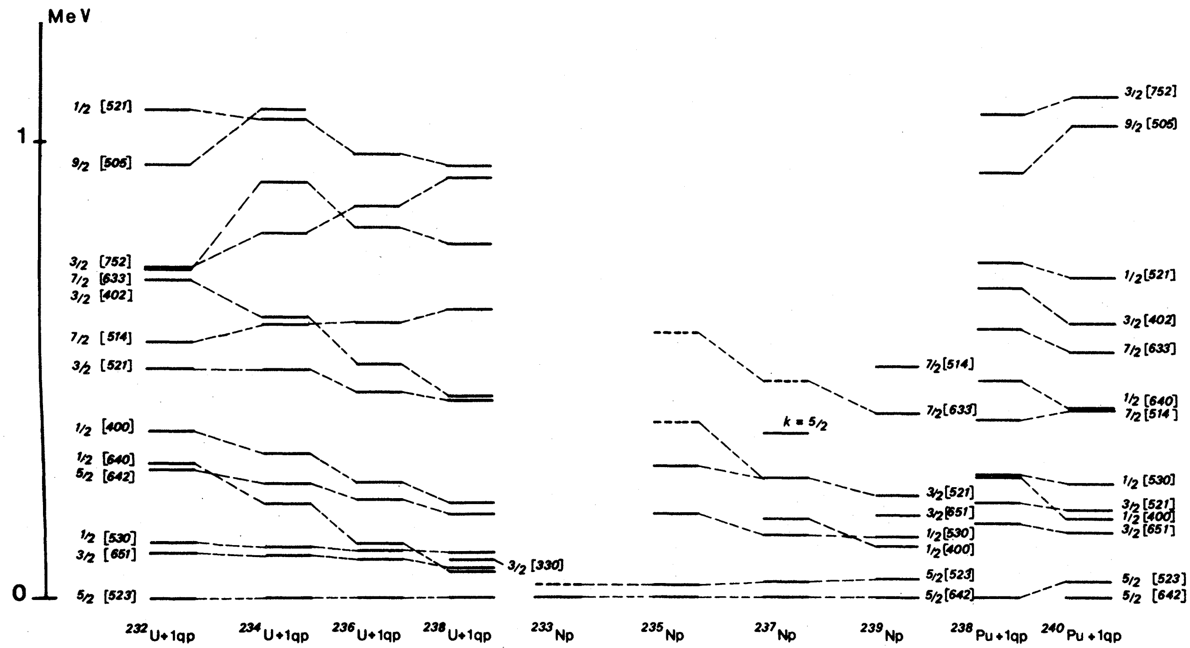

FIG. 4. Comparison of experimental energy band heads in ^{233,235,237,239}Np with those calculated in terms of one proton quasiparticle coupled to ^{232,234,236,238}U and ^{238,240}Pu cores.

Table II). We, therefore, suggest that the $\frac{1}{2}^+[640]$ assignment might be not correct (see also the discussion of Fig. 7 below) and rather of a $\frac{7}{2}^+[624]$ nature.

In Table II, we have listed for the ^{231}Th calculations using both ^{230}Th and ^{232}Th cores: (i) the main qp components for each band head state after

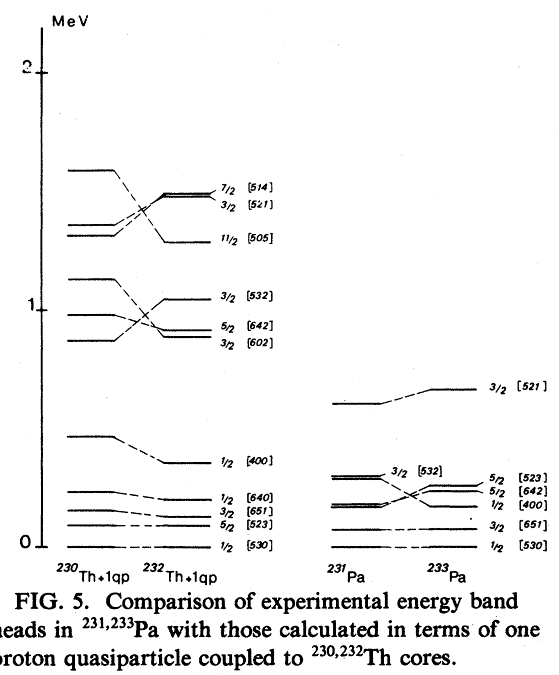

FIG. 5. Comparison of experimental energy band heads in ^{231,233}Pa with those calculated in terms of one proton quasiparticle coupled to ^{230,232}Th cores.

Coriolis mixing, and (ii) for each qp state the main asymptotic number basis components. From inspection of this table (and Tables IV and VI) one notices that sp states are in most cases far from being pure "asymptotic" states, as already found in other nuclear regions (see, e.g., Tables V and VI of Ref. 29) at all deformations including very large ones (see, e.g., Table I of Ref. 10). The latter often has the consequence that what is "experimentally" known, as for instance a $\frac{5}{2}^-[752]$ state, $\frac{1}{2}^-[501]$ state, or a $\frac{3}{2}^-[761]$ state is, in fact, made of 25% of the [532] state plus 24% of the [752] state, or 29% of the [701] state plus 24% of the [501] state, or even 25% of the [741] state plus 15% of the [981] state plus only 10% of the [761] state. It is also a remarkable fact that most of the considered bands are of an almost pure qp character (no Coriolis mixing). However, for some states one may observe significant differences in the Coriolis mixing rates when comparing the two theoretical descriptions using one core or another. This is particularly so for the $\frac{3}{2}^+[631]$ and $\frac{7}{2}^-[743]$ states.

Experimental ^{233}Th data[16,30] may be compared with the (^{232}Th + 1 qp) part of Fig. 6. As sketched on Fig. 7, out of the 17 known bands, nine have been considered so far as being of a pure rotational character. The latter is confirmed by our calculations which give most of them below 500 keV as

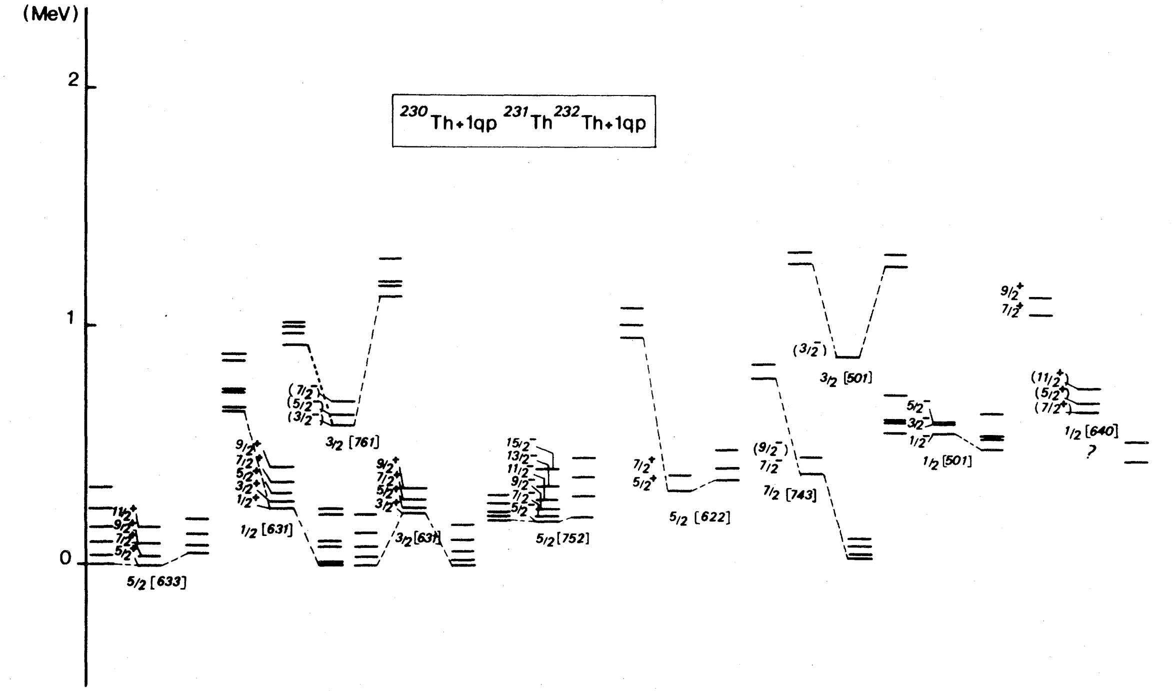

FIG. 6. Comparison of the full experimental level scheme of ^{231}Th with the theoretical results obtained when coupling one neutron quasiparticle to a ^{230}Th or ^{232}Th core. Results corresponding to the ^{230}Th and ^{232}Th core are reported on the left-hand or right-hand side of the experimental levels of each band.

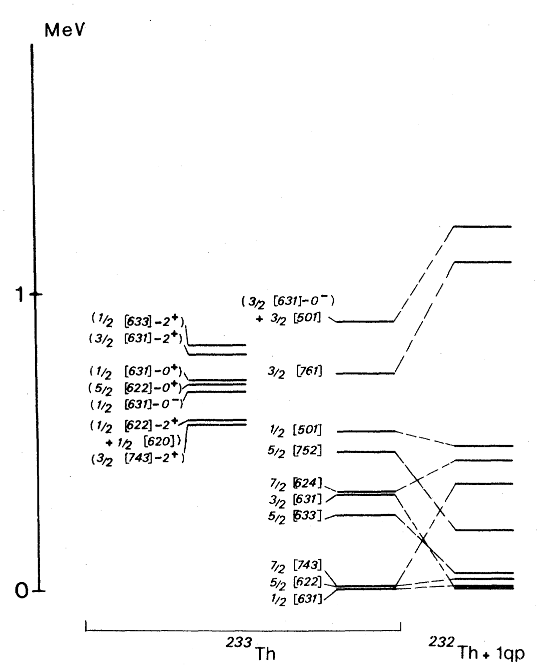

FIG. 7. Comparison of experimental energy band heads in ^{233}Th with those calculated in terms of one neutron quasiparticle coupled to a ^{232}Th core.

experimentally observed. In particular, one finds at the right energy the observed $\frac{7}{2}^+$[624] band which provides an indirect confirmation of the validity of our discussion about the so-called "$\frac{1}{2}^+$[640]" band in ^{231}Th. There are eight experimental bands left for only one theoretical band in the considered energy range. However, the band head state postulated to be of a $(\frac{3}{2}^-[501]+0^- * \frac{3}{2}^+[631])$ nature, found at 925 keV, seems to correspond to our $\frac{3}{2}^-$[501] band head state calculated at 1.24 MeV. It is also remarkable that the seven remaining bands found experimentally in the $0.1-1$ MeV range do *not* have any counterpart in our calculations, which provides an indirect but striking confirmation of their nonrotational character.

For the ^{229}Th nucleus, only three bands ($\frac{5}{2}^+$[633], $\frac{3}{2}^+$[631], and $\frac{1}{2}^+$[631]) are known experimentally. They are perfectly reproduced—see Table III—for the two lowest bands, whereas the third one is found slightly too high.

In ^{235}U below 1.1 MeV, 17 bands have been proposed out of which nine have been interpreted in terms of qp plus rotor states[15,20] and six in terms of qp-vibrator coupled states.[19] On Fig. 8 it is seen

TABLE III. Comparison between experimental and calculated energy levels of ^{229}Th. Theoretical results have been obtained by coupling one neutron qp to a ^{230}Th core. Energies are given in keV. Nuclear states are identified by their spin and parity I^π, and bands to which they belong in terms of the usual "experimental" $K^\pi[Nn_z\Lambda]$ assignment.

band	$\frac{5}{2}$[633]		$\frac{3}{2}$[631]		$\frac{1}{2}$[631]	
	exp	theor	exp	theor	exp	theor
$\frac{1}{2}^+$					262	650
$\frac{3}{2}^+$			<0.1	0	289	660
$\frac{5}{2}^+$	0	8	29	33		
$\frac{7}{2}^+$	43	48	72	80		
$\frac{9}{2}^+$	97	100	126	137		
$\frac{11}{2}^+$	163	165	196	213		
$\frac{13}{2}^+$	242	242				
$\frac{15}{2}^+$	327	333				

that we do reproduce the nine bands of the first type ($\frac{7}{2}^-$[743], $\frac{1}{2}^+$[631], $\frac{5}{2}^+$[633], $\frac{5}{2}^+$[622], $\frac{3}{2}^+$[631], $\frac{7}{2}^+$[624], $\frac{5}{2}^-$[752], $\frac{1}{2}^-$[501], $\frac{9}{2}^-$[734]). In two cases, the proposed[20] assignment as $\frac{7}{2}^+$[624] and $\frac{9}{2}^-$[734] bands is confirmed by our calculations. The absence in our results of six bands is consistent with their previous assignment as vibration coupling bands: $0^- * \frac{1}{2}^+$[631] at 761 keV, $0^+ * \frac{1}{2}^+$[631] at 769 keV, $2^+ * \frac{7}{2}^-$[743] at 638 keV, $2^+ * \frac{5}{2}^+$[622] at 843 keV, $0^+ * \frac{5}{2}^+$[622] at 905 keV, and $2^+ * \frac{3}{2}^+$[631] at 968 keV. Out of the 17 known bands, there are two remaining experimental bands.[19,20] One (at 806 keV) has been tentatively assigned in Ref. 19 as a Coriolis mixture of $\frac{3}{2}^-$[501] and $\frac{3}{2}^-$[741] qp states. We confirm it and suggest that the last experimental band

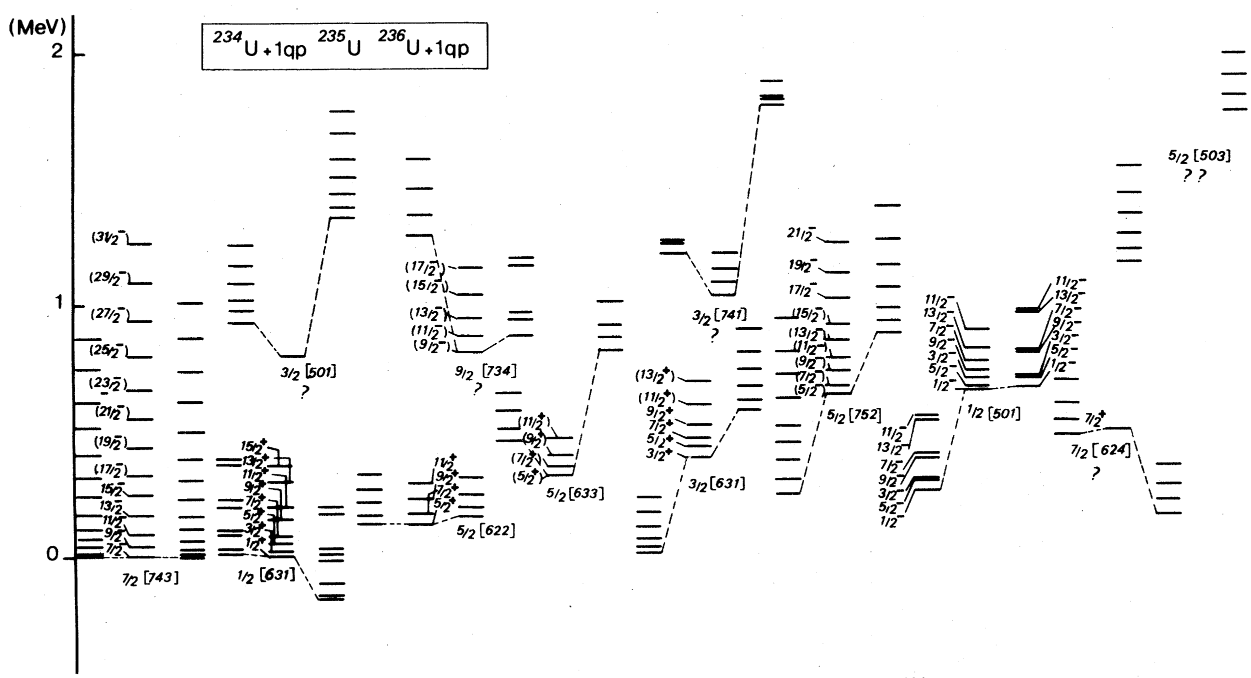

FIG. 8. Same as Fig. 6 for the ^{235}U nucleus. Results corresponding to the ^{234}U and ^{236}U core are reported on the left-hand or right-hand side of the experimental levels of each band.

TABLE IV. Same as Table II for the ^{235}U nucleus.

Usual assignment	^{234}U+1 qp calculations	^{236}U+1 qp calculations
$\frac{7}{2}^-[743]$	91% $\frac{7}{2}\{51\%[743]\}$	98% $\frac{7}{2}\{52\%[743]\}$
$\frac{1}{2}^+[631]$	100% $\frac{1}{2}\{28\%[631]+10\%[611]+8\%[431]+7\%[640]\}$	100% $\frac{1}{2}\{29\%[631]+9\%[611]+9\%[431]+7\%[640]\}$
$\frac{5}{2}^+[622]$	99% $\frac{5}{2}\{38\%[622]+12\%[422]\}$	99% $\frac{5}{2}\{39\%[622]+13\%[422]\}$
$\frac{5}{2}^+[633]$	99% $\frac{5}{2}\{57\%[633]\}$	100% $\frac{5}{2}\{58\%[633]\}$
$\frac{3}{2}^+[631]$	92% $\frac{3}{2}\{30\%[631]+11\%[431]+10\%[611]\}$	100% $\frac{3}{2}\{30\%[631]+12\%[431]+10\%[611]\}$
$\frac{5}{2}^-[752]$	99% $\frac{5}{2}\{34\%[752]+24\%[732]\}$	98% $\frac{5}{2}\{35\%[752]+23\%[732]\}$
$\frac{1}{2}^-[501]$	100% $\frac{1}{2}\{30\%[501]+29\%[701]\}$	100% $\frac{1}{2}\{30\%[701]+30\%[501]\}$
$\frac{9}{2}^-[734]$	80% $\frac{9}{2}\{64\%[734]\}$	94% $\frac{9}{2}\{65\%[734]\}$
$\frac{3}{2}^-[501]$	73% $\frac{3}{2}\{26\%[701]+24[501]\}$	80% $\frac{3}{2}\{19\%[701]+18\%[501]+15\%[301]\}$
	+ 27% $\frac{3}{2}\{20\%[741]+16\%[761]+11\%[981]+9\%[752]\}$	+ 20% $\frac{3}{2}\{21\%[741]+11\%[701]+11\%[761]+9\%[501]\}$
$\frac{3}{2}^-[741]$	71% $\frac{3}{2}\{20\%[741]+16\%[761]+11\%[981]+9\%[752]\}$	75% $\frac{3}{2}\{21\%[741]+11\%[701]+11\%[761]+9\%[501]\}$
	+ 26% $\frac{3}{2}\{26\%[701]+24\%[501]\}$	+ 19% $\frac{3}{2}\{19\%[701]+18\%[501]+15\%[301]\}$
$\frac{7}{2}^+[624]$	93% $\frac{7}{2}\{68\%[624]\}$	96% $\frac{7}{2}\{69\%[624]\}$
$\frac{5}{2}^-[503]$	95% $\frac{5}{2}\{44\%[503]+25\%[703]\}$	99% $\frac{5}{2}\{44\%[503]+25\%[703]\}$

should correspond to the calculated band exhibiting a roughly inverse mixing ratio of the two above listed qp states. The first calculated band not connected with any experimentally seen band structure originates from a $\frac{5}{2}^-[503]$ qp state and has been calculated at $\sim 1.2-1.6$ MeV (depending on the choice of the core).

As mentioned in the discussion of Table II, the calculated sp states are generally very much mixed with respect to the basis states. This conclusion holds in the case of ^{234}U and ^{236}U core sp states (see Table IV). For instance, the so-called $\frac{3}{2}^+[631]$ is in fact a mixture: $30\%[631]+11\%[431]+\ldots$. Besides, the qp mixing is found very weak (with the exceptions of the two $\frac{3}{2}^-$ bands discussed above) as shown also in Table IV. By merely inspecting the Coriolis mixing rates, one is able to identify the members of a given band provided that they are not perturbed too much by the rotation-particle coupling term. This point is illustrated in Table V for the typical examples of the $\frac{1}{2}^+[631]$ and $\frac{7}{2}^-[743]$ bands in ^{235}U.

TABLE V. Percentage of the major qp component in two bands of ^{235}U calculated within the $^{236}U+1$ qp approximation. As seen on Table IV, the major qp component for the $\frac{7}{2}^-[743]$ band states is a $\frac{7}{2}^-$ qp state made of 52% of the [743] asymptotic basis state, whereas a mixture of [631], [611], [431], [640], etc, . . . $\frac{1}{2}^+$ states constitutes the major qp component of the $\frac{1}{2}^+[631]$ band states.

$\frac{7}{2}^-[743]$ band		$\frac{1}{2}^+[631]$ band	
$\frac{7}{2}-$	98%	$\frac{1}{2}+$	100%
$\frac{9}{2}-$	95%	$\frac{3}{2}+$	99.9%
$\frac{11}{2}-$	91%	$\frac{5}{2}+$	99.7%
$\frac{13}{2}-$	88%	$\frac{7}{2}+$	99.6%
$\frac{15}{2}-$	85%	$\frac{9}{2}+$	99.2%
$\frac{17}{2}-$	82%	$\frac{11}{2}+$	99.1%
$\frac{19}{2}-$	79%	$\frac{13}{2}+$	98.7%
$\frac{21}{2}-$	77%	$\frac{15}{2}+$	98.5%
$\frac{23}{2}-$	75%		
$\frac{25}{2}-$	73%		
$\frac{27}{2}-$	71%		
$\frac{29}{2}-$	70%		

In ^{239}Np, there are five confirmed experimental[15] bands, which are well reproduced by our calculations (see Fig. 9). However, the ground state band ordering is rather poorly reproduced in the ^{238}U calculations which seems to be due to its strongly mixed character (see Table VI). We confirm the tentative assignments of two bands ($\frac{3}{2}^+[651]$ and $\frac{7}{2}^+[633]$). The first of these two bands is strongly perturbed, when calculated with the ^{238}U core solutions with a band head energy, however, which is estimated somewhat too low (by ~ 0.7 MeV). Another band has been tentatively assigned as a $\frac{1}{2}^+[400]$ band. We do confirm its $\frac{1}{2}$ character but we fail to confirm the asymptotic quantum number labeling, since the $\frac{1}{2}^+[400]$ state constitutes only 4% (10%, respectively) of the major qp state component coupled to the ^{238}U (^{240}Pu, respectively) core. As already noted in the discussion of Fig. 4, the band head locations are better reproduced in ^{240}Pu core calculations than in ^{238}U core calculations.

So far all the results which have been discussed have been obtained with a variable moment of inertia $\mathscr{I}(R)$ deduced from the energy level sequence in the ground state bands of adjacent even-even nuclei. We would like now to check how sensitive the calculational results are with respect to this choice. For this purpose we have repeated some of the calculations with a constant moment of inertia deduced from the first 2^+ excitation energy. Moreover, since we have at our disposal some Inglis cranking values $\mathscr{I}_{cr}$ (see Table I) we have also repeated the same calculations with these cranking moments of inertia. In Table VII we have compared for three bands ($\frac{5}{2}^+[633]$ and $\frac{3}{2}^+[631]$ in $^{230}Th+1$ qp, and $\frac{7}{2}^-[743]$ in $^{236}U+1$ qp) the energy level sequences calculated with $\mathscr{I}_0$, $\mathscr{I}(R)$, and $\mathscr{I}_{cr}$. We observe for these rather pure bands no significant differences between the three sets of results. In cases where there exists some significant amount of Coriolis mixing, the same conclusion seems to hold not only for the energies but for the qp content of the band states also, as exemplified in Table VIII for the two lowest $\frac{3}{2}^-$ bands found in the $^{236}U+1$ qp calculations. It is, therefore, not surprising that when calculating a whole nuclear spectrum with a constant moment of inertia equal to $\mathscr{I}_{cr}$, we get the same qualitative results as those obtained with $\mathscr{I}(R)$ as shown on Fig. 10 for the ^{235}U nucleus. This figure is indeed very close to the corresponding Fig. 8 [using $\mathscr{I}(R)$]. In the $\mathscr{I}_{cr}$ calculations we reproduce reasonably well the nine confirmed rotational

TABLE VI. Same as Table II for the ^{239}Np nucleus.

Usual assignment	^{238}U+1 qp calculations	^{240}Pu+1 qp calculations
$\frac{5}{2}^+[642]$	$74\%\ \frac{5}{2}\{37\%[642]+19\%[622]\}$	$93\%\ \frac{5}{2}\{33\%[642]+19\%[862]\}$
	$+\ 19\%\ \frac{1}{2}\{25\%[600]+22\%[200]+17\%[400]\}$	
	$+\ 7\%\ \frac{3}{2}\{24\%[631]+19\%[651]+15\%[871]\}$	
$\frac{5}{2}^-[523]$	$99.9\%\ \frac{5}{2}\{65\%[523]\}$	$99.9\%\ \frac{5}{2}\{63\%[523]\}$
$\frac{1}{2}^+[400]$	$83\%\ \frac{1}{2}\{12\%[640]+11\%[620]+11\%[631]+8\%[651]+8\%[200]\}$	$92\%\ \frac{1}{2}\{17\%[200]+14\%[600]+10\%[620]+10\%[400]\}$
	$+\ 17\%\ \frac{1}{2}\{25\%[600]+22\%[200]+17\%[400]\}$	
$\frac{1}{2}^-[530]$	$99.9\%\ \frac{1}{2}\{22\%[330]+16\%[530]+13\%[750]\}$	$99\%\ \frac{1}{2}\{21\%[330]+16\%[530]+13\%[750]\}$
$\frac{3}{2}^+[651]$	$75\%\ \frac{3}{2}\{24\%[631]+19\%[651]+15\%[871]\}$	$95\%\ \frac{3}{2}\{24\%[631]+17\%[871]+16\%[651]\}$
	$+\ 23\%\ \frac{1}{2}\{12\%[640]+11\%[620]+11\%[631]+8\%[651]+8\%[200]\}$	
$\frac{3}{2}^-[521]$	$99\%\ \frac{3}{2}\{31\%[521]+21\%[321]\}$	$94\%\ \frac{3}{2}\{29\%[521]+21\%[321]\}$
$\frac{7}{2}^+[633]$	$99\%\ \frac{7}{2}\{54\%[633]\}$	$99\%\ \frac{7}{2}\{51\%[633]\}$
$\frac{7}{2}^-[514]$	$99.8\%\ \frac{7}{2}\{74\%[514]\}$	$99\%\ \frac{7}{2}\{72\%[514]\}$

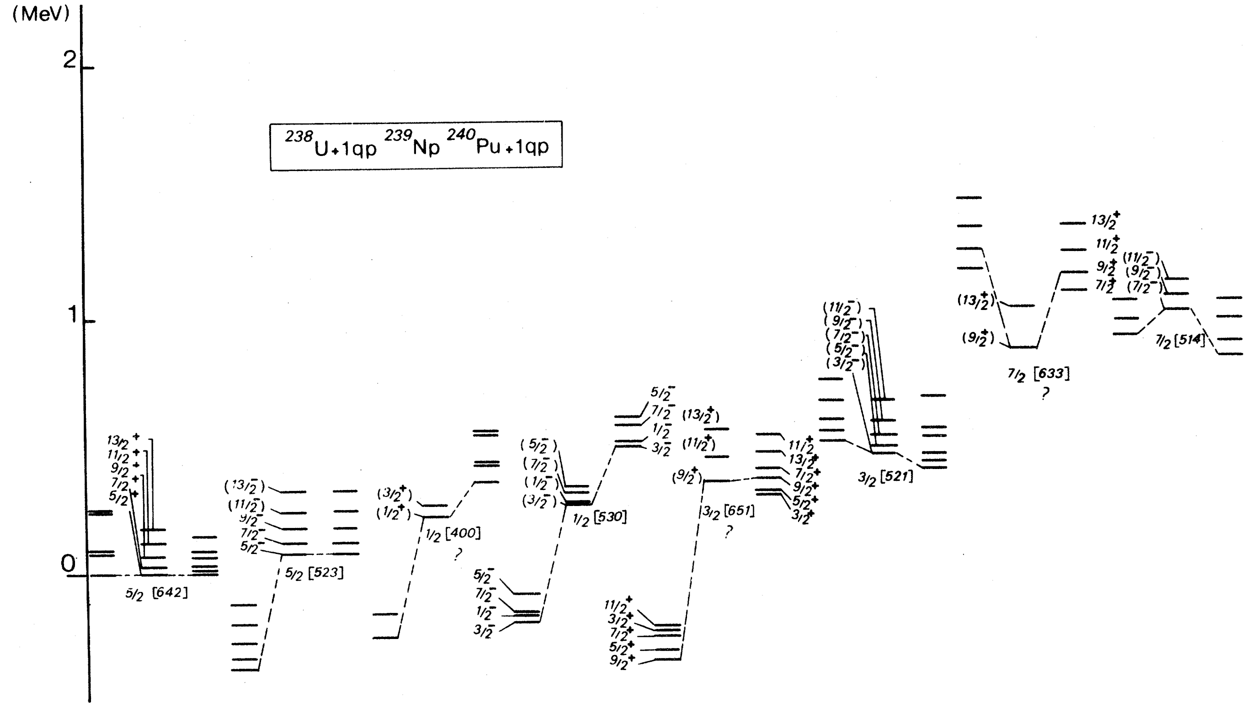

FIG. 9. Same as Fig. 6 for the ^{239}Np nucleus. Results corresponding to the ^{238}U and ^{240}Pu core are reported on the left-hand or right-hand side of the experimental levels of each band.

bands which are known in this nucleus. The latter is rather remarkable in view of the fact that in this case we have only six force parameters and two pairing gaps as phenomenological inputs.

IV. $E2$ AND $M1$ PROPERTIES

Experimental[15,16,31] magnetic dipole and electric quadrupole moments obtained by several techniques are compared in Tables IX and X with theoretical values.

In order to investigate the influence of poorly known polarization effects, two values of the spin gyromagnetic ratio ($g_s = g_s^{\text{free}}$ and $0.6\, g_s^{\text{free}}$) have been considered. The calculated values are generally in rather good agreement with experimental data, indeed much more so for protons than for neutrons as already found in other calculations. Our results have also been compared with those obtained in a somewhat more phenomenological approach due to Chasman *et al.*[17] In this reference one may note, for instance, that a marked disagreement between experimental and calculated magnetic moment was obtained for the neutron $\frac{5}{2}^+[622]$ and the proton $\frac{1}{2}^-[530]$ orbitals, whereas we reproduce rather well the data for both states.

As for the electric quadrupole moments, our calculational results also agree with experimental results without any *ad hoc* effective charge adjustment of the $E2$ operator. This is in fact not very surprising, since the particle (intrinsic) contribution is negligible, the core contribution plays the prominent role and has been shown in I to be fairly well represented in our HF plus BCS calculations.

A further step in the characterization of the single-particle part of our wave functions consists in studying the reduced $E2$ and $M1$ transition probabilities to which they lead. In this heavy nuclei region, in contrast with the large wealth of experimental results concerning energy levels, there are rather few absolute transition probabilities available from lifetime measurements or Coulomb excitation experiments.

As seen in Table XI, absolute $M1$ and $E2$ *intraband* transitions measured in several nuclei[16,32–36] are fairly well described in our calculations. A reproduction of transition probability ratios is rather easy to obtain since they are (as often pointed

TABLE VII. Comparison of energy level sequences within given bands when calculated with three different prescriptions for the moment of inertia [$\mathscr{I}_0$, $\mathscr{I}(R)$, $\mathscr{I}_{cr}$] defined in the text. Energies are given in MeV. In the three cases considered here the bands correspond to almost pure qp configurations.

	$\frac{5}{2}[633]$ in ^{230}Th+1 qp		
	$\mathscr{I}_0$	$\mathscr{I}_{(R)}$	$\mathscr{I}_{cr}$
$\frac{5}{2}+$	0.01	0.01	0.02
$\frac{7}{2}+$	0.05	0.05	0.07
$\frac{9}{2}+$	0.11	0.10	0.15
$\frac{11}{2}+$	0.19	0.17	0.24
$\frac{13}{2}+$	0.27	0.24	0.35
$\frac{15}{2}+$	0.37	0.33	0.49
	$\frac{3}{2}[631]$ in ^{230}Th+1 qp		
	$\mathscr{I}_0$	$\mathscr{I}_{(R)}$	$\mathscr{I}_{cr}$
$\frac{3}{2}+$	0	0	0
$\frac{5}{2}+$	0.04	0.03	0.05
$\frac{7}{2}+$	0.09	0.08	0.11
$\frac{9}{2}+$	0.15	0.14	0.20
$\frac{11}{2}+$	0.24	0.21	0.31
	$\frac{7}{2}[743]$ in ^{236}U+1 qp		
	$\mathscr{I}_0$	$\mathscr{I}_{(R)}$	$\mathscr{I}_{cr}$
$\frac{7}{2}-$	0	0	0
$\frac{9}{2}-$	0.03	0.01	0.03
$\frac{11}{2}-$	0.07	0.03	0.06
$\frac{13}{2}-$	0.12	0.06	0.12
$\frac{15}{2}-$	0.18	0.11	0.18

out) roughly fulfilling the Alaga rules. More important, therefore, is the agreement obtained here for absolute intraband transitions (e.g., for the $\frac{5}{2}^+[633]$, $\frac{3}{2}^+[631]$, $\frac{1}{2}^+[631]$ neutron and $\frac{1}{2}^-[530]$, $\frac{5}{2}^+[642]$ proton bands).

Interband transition measurements are very difficult to perform. In Table XII we have compared such calculated and experimental $M1$ and $E2$ transition probabilities.[34,37,38] In the ^{231}Pa case we present $\Delta K=1$ interband transition probability ratios. These results show that without any attenuation factor, the quality of our wave functions is sufficient to guarantee a good agreement with the corresponding data. The absolute $\Delta K=2$ interband transition probabilities of Table XII (between $\frac{5}{2}^+[622]$ and $\frac{1}{2}^+[631]$ band states) constitute a far more stringent test: for $E2$ transitions, we have obtained about the right order of magnitude for $M1$ transitions, whereas experimental retardation factors relative to standard spherical single-particle estimates ranged from 10^3 to 10^4, we have reduced these factors to about 10.

In Tables XIII and XIV we have performed a detailed comparison of theoretical and experimental[15,39] absolute $E2$ and relative $M1$ reduced transition probabilities in the particular case of the well documented ^{235}U nucleus [incidentally, it may be mentioned that *absolute* determinations of $B(E2)$ probabilities from Coulomb excitation experiments are not always free from possible systematic errors]. Intraband $\frac{7}{2}^-[743]$ $E2$ transitions, as well as $\Delta K=1$ interband transitions connecting the $\frac{7}{2}^-[743]$ ground state band to the $\frac{5}{2}^-[752]$ and $\frac{9}{2}^-[734]$ bands, are well reproduced by our calculations (see Table XIII). In the lower part of this table we provide a striking evidence of the nonrotational character of the $\frac{3}{2}^-$ band (located at 638 keV above the ground state). A possible rotor plus qp candidate might have been the $\frac{3}{2}^-[501]$ band. With this assignment, however, it is impossible to reproduce the rather high $B(E2)$ value for the (g.s. band $\to\frac{3}{2}^-$ band) transition. Thus our results are consistent with the assignment of the $\frac{3}{2}^-$ state as being of a vibration coupling state (namely a $\frac{7}{2}^-[743]*2_\gamma^+$).

In Table XV we have shown, for two typical examples, the influence of our choice for the core gyromagnetic factor g_R. From these examples it can be seen that the variation of magnetic properties due to a $\sim 30\%$ change in g_R (from Z/A to the Inglis cranking formula value) is roughly of the same order of magnitude as the variation due to polarization effects on g_s factors.

V. CONCLUSIONS

The rotor plus quasiparticle approximation is a rather old one and within this framework many results have been previously reported in heavy nuclei as well as in light nuclei (see, e.g., Refs. 17 and 40). However, all these approaches are purely

TABLE VIII. Comparison of energy level sequences within strongly Coriolis coupled bands in ^{236}U+1 qp calculations with three different prescriptions for the moment of inertia [$\mathscr{I}_0$, $\mathscr{I}(R)$, $\mathscr{I}_{cr}$] defined in the text. Energies E are given in keV. The bands result mostly from the coupling of two $\frac{3}{2}^-$ qp states [A] and [B] specified by [A]=19%[701]+18%[501]+15%[301] and [B]=21%[741]+11%[701]+11%[761]+9%[501]. In the columns labeled [A] and [B] one reads the Coriolis mixing rates (percentage). For the $\frac{7}{2}$ and $\frac{11}{2}$ spins, the [A] and [B] qp states are shared between three different nuclear states.

	$\mathscr{I}_0$			$\mathscr{I}(R)$			$\mathscr{I}_{cr}$		
	E	[A]	[B]	E	[A]	[B]	E	[A]	[B]
$\frac{3}{2}^-$	1340	79	21	1352	80	20	1244	77	23
	1775	19	74	1775	19	75	1771	20	69
$\frac{5}{2}^-$	1378	78	21	1389	79	20	1292	75	24
	1817	19	74	1813	18	75	1833	20	69
	1429	78	20	1439	79	20	1358	74	23
$\frac{7}{2}^-$	1794	11	56	1794	11	59	1775	9	45
	2230	9	21	2214	8	19	2299	12	28
$\frac{9}{2}^-$	1542	76	22	1505	77	21	1446	71	25
	1933	16	67	1917	16	69	1994	17	59
	1575	75	19	1580	77	18	1548	69	23
$\frac{11}{2}^-$	1847	4	41	1841	4	46	1842	3	29
	2440	14	33	2393	13	31	2601	17	37
$\frac{13}{2}^-$	1676	72	23	1676	74	21	1677	66	26
	2137	14	59	2083	14	63	2259	14	49

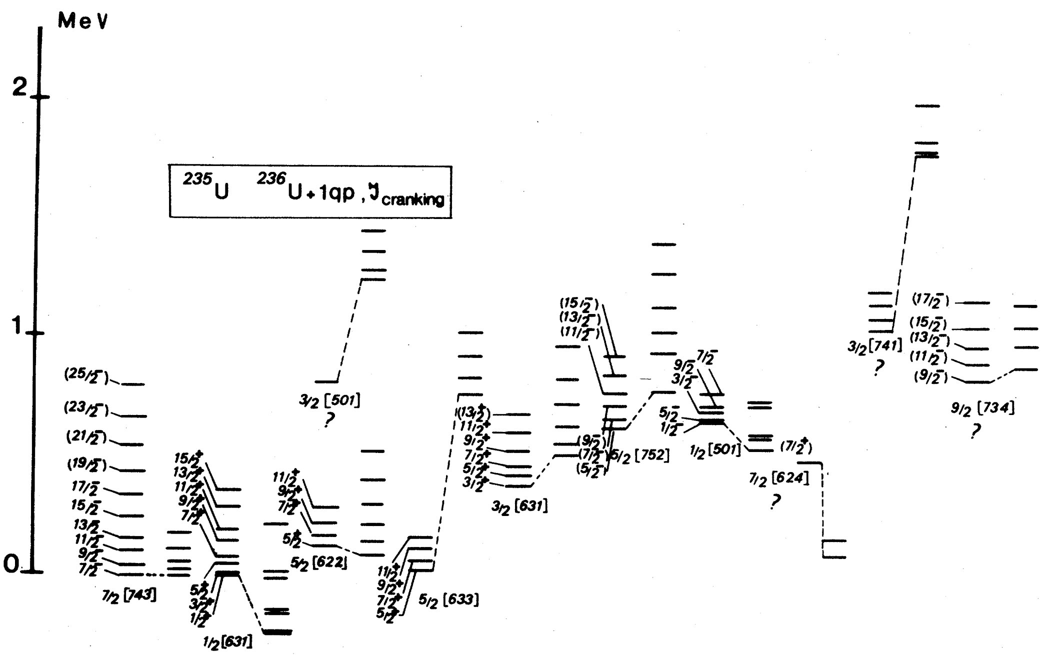

FIG. 10. Same as Fig. 8 when using, instead of the variable moment of inertia $\mathscr{I}(R)$, the Inglis cranking value $\mathscr{I}_{cr}$ determined from HF plus BCS results in Ref. 7.

TABLE IX. Comparison between experimental and theoretical magnetic moments (expressed in nuclear magneton μ_N). In this table as in the following ones, experimental figures marked by an asterisk indicate that the value is contingent upon another experimental moment. Our calculated values are displayed on two lines. For a nucleus whose nucleon number is A, the upper and lower one corresponds to a $(A+1)$ core+1 qp [$(A-1)$ core+1 qp, respectively] calculation. The moment has been evaluated with $g_s = 0.6 g_s^{\text{free}}$, whereas the figure given in parentheses corresponds to $g_s = g_s^{\text{free}}$. In some cases we have also given the moments obtained in the phenomenological approach of Ref. 17.

Nucleus	Spin	Usual assignment	Experimental	Reference	This work	Other calculations[17]
			0.46 ±0.04*	a		
^{229}Th	$\frac{5}{2}$	$\frac{5}{2}^+[633]$	0.42 ±0.10	a	0.71(1.03)	0.43−0.59
			0.35 ±0.07	a		
^{233}U	$\frac{5}{2}$	$\frac{5}{2}^+[633]$	0.55	a	0.69(0.99)	
			0.73	a	0.47(0.44)	
			0.64	b		
			−0.35	a		
^{235}U	$\frac{7}{2}$	$\frac{7}{2}^-[743]$	−0.36	a	−0.57(−1.26)	−0.23
			−0.43	b	−0.77(−1.26)	
^{239}Pu	$\frac{1}{2}$	$\frac{1}{2}^+[631]$	0.203±0.040	a	0.23(0.23)	0.2−0.23
			0.200	b	0.22(0.23)	
	$\frac{5}{2}$	$\frac{5}{2}^+[622]$	−1.25 ±0.29	a	−0.39(−0.81)	
					−0.40(−0.82)	
			−0.683±0.015*	a	−0.39(−0.81)	
^{241}Pu	$\frac{5}{2}$	$\frac{5}{2}^+[622]$	−0.728±0.017*	a		−0.23− −0.03
			−0.714±0.019	a		
^{231}Pa	$\frac{3}{2}$	$\frac{1}{2}^-[530]$	2.01 ±0.02	a	2.26(3.24)	0.76−0.78
					2.24(3.22)	
^{233}Pa	$\frac{3}{2}$	$\frac{1}{2}^-[530]$	3.5 ±0.8	a	2.27(2.52)	
					2.25(2.50)	
			3.14 ±0.04	a	3.23(3.89)	
^{237}Np	$\frac{5}{2}$	$\frac{5}{2}^+[642]$	3.3 ±0.9	a	4.59(5.51)	2.50−2.51
			~2.9	a		
			1.95 ±0.15	a	1.46(0.82)	
	$\frac{5}{2}$	$\frac{5}{2}^-[523]$	1.34 ±0.12	b	1.45(0.83)	
			1.68 ±0.03*	a		

TABLE IX. (*Continued*.)

Nucleus	Spin	Usual assignment	Experimental	Reference	This work	Other calculations[17]
^{239}Np	$\frac{5}{2}$	$\frac{5}{2}^{+}[642]$	2.03 $\pm$0.25	a	1.45(0.82) 1.45(0.82)	
^{241}Am	$\frac{5}{2}$	$\frac{5}{2}^{-}[523]$	1.61 $\pm$0.03 1.59	a b	1.45(0.82)	1.56–1.57

[a]Experimental data are extracted from Ref. 31.
[b]Experimental data are extracted from Refs. 15 and 16.

TABLE X. Same as Table IX for quadrupole moments (expressed in barn). In particular note that the lower and upper calculated moments correspond to $(A-1)$ and $(A+1)$ core calculations.

Nucleus		Usual assignment	Experimental	Reference	This work
^{229}Th	$\frac{5}{2}$	$\frac{5}{2}^{+}[633]$	4.3 $\pm$0.9 $\sim$4.6	a a	2.72
^{233}U	$\frac{5}{2}$	$\frac{5}{2}^{+}[633]$	3.5 4.2 7.9	a b a	3.5 2.5
^{235}U	$\frac{7}{2}$	$\frac{7}{2}^{-}[743]$	4.55$\pm$0.09 4.1 4.9	a a b	4.6 4.2
^{241}Pu	$\frac{5}{2}$	$\frac{5}{2}^{+}[622]$	5.6 $\pm$2.0	a	4.0
^{233}Pa	$\frac{3}{2}$	$\frac{1}{2}^{-}[530]$	-3.0	a	-1.9 -1.8
^{237}Np	$\frac{5}{2}$	$\frac{5}{2}^{+}[642]$	4.1 $\pm$0.7* 3.7 $\pm$0.8	a b	-1.2 3.7
	$\frac{5}{2}$	$\frac{5}{2}^{-}[523]$ (relative to $\frac{5}{2}^{+}[642]$)	1.0 $\pm$0.1	b	1.06 0.97
^{241}Am	$\frac{5}{2}$	$\frac{5}{2}^{-}[523]$	4.9	a	4.0

[a]Experimental data extracted from Ref. 31.
[b]Experimental data extracted from Refs. 15 and 16.

TABLE XI. Comparison of experimental and calculated intraband $E2$ and $M1$ reduced transition probabilities [$B(E2)$ are expressed in $e^2\,\mathrm{fm}^4$ and $B(M1)$ in $\mu_N{}^2$]. We have also given δ^2 E2-$M1$ mixing ratios, defined as $\delta^2=T_\gamma(E2)/T_\gamma(M1)$ (with usual notation).

^{229}Th	$B(E2;\frac{7}{2}\rightarrow\frac{5}{2})$	$(2.70\ \pm0.23)\ 10^4$ $(2.41\ \pm0.22)\ 10^4$	^{230}Th+1 qp	(2.44)	10^4
$\frac{5}{2}$[633][a]	$B(E2;\frac{9}{2}\rightarrow\frac{5}{2})$	$(0.63\ \pm0.10)\ 10^4$	^{230}Th+1 qp	(0.79)	10^4
	$B(E2;\frac{9}{2}\rightarrow\frac{7}{2})$	$(2.27\ \pm0.40)\ 10^4$	^{230}Th+1 qp	(1.97)	10^4
	$B(M1;\frac{7}{2}\rightarrow\frac{5}{2})$	0.0134 ± 0.0022 0.0185 ± 0.0025	^{230}Th+1 qp	0.0092	
	$B(M1;\frac{9}{2}\rightarrow\frac{7}{2})$	0.0228 ± 0.0062	^{230}Th+1 qp	0.013	
	$\delta^2(\frac{9}{2}\rightarrow\frac{7}{2})$	$0.33\ \pm0.05$ $0.25\ \pm0.04$	^{230}Th+1 qp	0.26	
	$\delta^2(\frac{11}{2}\rightarrow\frac{9}{2})$	$0.32\ \pm0.04$ $0.17\ \pm0.06$	^{230}Th+1 qp	0.17	
	$\delta^2(\frac{13}{2}\rightarrow\frac{11}{2})$	$0.5\ \pm0.2$	^{230}Th+1 qp	0.27	
$\frac{3}{2}$[631]	$\delta^2(\frac{9}{2}\rightarrow\frac{7}{2})$	$0.027\ \pm0.06$	^{230}Th+1 qp	0.023	
	$\delta^2(\frac{11}{2}\rightarrow\frac{9}{2})$	$0.028\ \pm0.04$	^{230}Th+1 qp	0.035	
^{231}Pa $\frac{1}{2}$[530][b]	$B(E2;\frac{7}{2}\rightarrow\frac{3}{2})$	$(1.89\ \pm0.12)\ 10^4$	^{230}Th+1 qp ^{232}U+1 qp	(1.87) (2.40)	10^4 10^4
^{233}U	$B(E2;\frac{5}{2}\rightarrow\frac{7}{2})$	$(0.5\ \pm0.3)\ 10^5$ $(1.2\ \pm0.2)\ 10^5$	^{234}U+1 qp	(0.45)	10^5
$\frac{5}{2}$[633][c]	$B(E2;\frac{5}{2}\rightarrow\frac{9}{2})$	$(0.238\ \pm0.014)\ 10^5$	^{234}U+1 qp	(0.89)	10^4
^{237}Np $\frac{5}{2}$[642][c]	$B(E2;\frac{5}{2}\rightarrow\frac{7}{2})$	$(0.45^{+0.06}_{-0.09})\ 10^5$	^{238}Pu+1 qp	(0.55)	10^5
	$B(E2;\frac{5}{2}\rightarrow\frac{9}{2})$	$(0.24\ \pm0.04)\ 10^5$	^{238}Pu+1 qp	(0.21)	10^5
^{239}Pu $\frac{1}{2}$[631][c]	$B(E2;\frac{1}{2}\rightarrow\frac{5}{2})$	$(0.53\ \pm0.03)\ 10^5$ $(0.44\ \pm0.03)\ 10^5$	^{238}Pu+1 qp ^{240}Pu+1 qp	(0.73) (0.74)	10^5 10^5

[a]Experimental data are taken from Refs. 16, 32, and 33.
[b]Experimental data are taken from Ref. 34.
[c]Experimental data are taken from Ref. 35.
[d]Experimental data are taken from Ref. 36.

TABLE XII. Same as Table XI for $\Delta K=1$ and $\Delta K=2$ interband transitions. For the ^{231}Pa data only relative $B(M1)$ values are given.

$\Delta K=1$ transitions

^{231}Pa					
$\frac{5}{2}[642]\rightarrow\frac{3}{2}[651]$	$B(M1;\frac{5}{2}\rightarrow\frac{3}{2})$	1.0	a	^{232}U+1 qp	1.0
	$B(M1;\frac{5}{2}\rightarrow\frac{5}{2})$	0.059 ± 0.005	a	^{232}U+1 qp	0.025
	$B(M1;\frac{5}{2}\rightarrow\frac{7}{2})$	$0.43^{+0.04}_{-0.05}$	a	^{232}U+1 qp	0.42
	$B(M1;\frac{7}{2}\rightarrow\frac{5}{2})$	1.0	a	^{232}U+1 qp	1.0
	$B(M1;\frac{7}{2}\rightarrow\frac{7}{2})$	0.17 ± 0.05	a	^{232}U+1 qp	0.478
	$B(M1;\frac{7}{2}\rightarrow\frac{9}{2})$	$0.83^{+0.22}_{-0.17}$	a	^{232}U+1 qp	0.257

$\Delta K=2$ transitions

^{239}U $\frac{5}{2}[622]\rightarrow\frac{1}{2}[631]$	$B(E2;\frac{5}{2}\rightarrow\frac{1}{2})$	1.17 ± 0.06	b	^{238}U+1 qp	24		
^{239}Pu	$B(M1;\frac{5}{2}\rightarrow\frac{7}{2})$	$(1.36\pm0.08)10^{-4}$	c	^{238}Pu+1 qp	$(11)10^{-4}$	^{240}Pu+1 qp	$(22)10^{-4}$
$\frac{5}{2}[622]\rightarrow\frac{1}{2}[631]$	$B(M1;\frac{5}{2}\rightarrow\frac{5}{2})$	$(3.53\pm0.21)10^{-4}$	c	^{238}Pu+1 qp	$(37)10^{-4}$	^{240}Pu+1 qp	$(25)10^{-4}$
	$B(M1;\frac{5}{2}\rightarrow\frac{3}{2})$	$(2.29\pm0.14)10^{-4}$	c	^{238}Pu+1 qp	$(25)10^{-4}$	^{240}Pu+1 qp	$(9)10^{-4}$
	$B(E2;\frac{5}{2}\rightarrow\frac{7}{2})$	0.64 ± 0.32	c	^{238}Pu+1 qp	1.8	^{240}Pu+1 qp	12.5
	$B(E2;\frac{5}{2}\rightarrow\frac{5}{2})$	1.00 ± 0.65	c	^{238}Pu+1 qp	3	^{240}Pu+1 qp	50
	$B(E2;\frac{5}{2}\rightarrow\frac{3}{2})$	1.27 ± 0.27	c	^{238}Pu+1 qp	0.09	^{240}Pu+1 qp	2.37
	$B(E2;\frac{5}{2}\rightarrow\frac{1}{2})$	2.15 ± 0.13	c	^{238}Pu+1 qp	0.89	^{240}Pu+1 qp	9.2
^{241}Pu $\frac{5}{2}[622]\rightarrow\frac{1}{2}[631]$	$B(E2;\frac{5}{2}\rightarrow\frac{1}{2})$	0.65 ± 0.08	b	^{240}Pu+1 qp	9.2		

[a]Experimental data are taken from Ref. 34.
[b]Experimental data are taken from Ref. 37.
[c]Experimental data are taken from Ref. 38.

phenomenological and involve, in general, some amount of *ad hoc* parametrization. Our approach on the other hand, as discussed in subsection II B, implies only six effective force parameters (valid for all nuclei and determined from other nuclear properties) supplemented by pairing gaps, and moments of inertia thus exluding any renormalization of the Coriolis coupling term (as, e.g., in approaches using so-called attenuation factors). Our work which undoubtedly constitutes an improvement on existing rotor plus qp calculations due in particular to the quality of the qp states in use, is not, however, free from the general drawbacks of the rotor plus qp approximation. The latter, intimately connected with an approximate projected HF treatment,[6] should only be justified in cases where the concept of a perfectly rigid rotating core is valid. In this respect, the present work should be considered only as a first step towards a more comprehensive treatment of the coupling between core and individual particle degrees of freedom. Recent progresses[41] in the treatment of the even-even core collective low energy dynamics will allow us in the near future to improve the presently rather crude core wave functions. Moreover, as pointed out by many authors, an independent particle approximation is rather

TABLE XIII. Comparison of experimental (Refs. 15, 39) and calculated $B(E2)$ reduced transitions probabilities in ^{235}U (expressed in e^2fm^4). All transitions originate from the ground state. Theoretical values are given for both core calculations. The last lines correspond to calculations performed to check whether the "experimental" $\frac{3}{2}^-(\frac{7}{2}^-[743]*2_\gamma^+)$ band might be a $\frac{3}{2}^-[501]$ band. The answer is negative.

Usual assignment	Final state spin and parity	Experimental	$^{234}U+1$ qp	$^{236}U+1$ qp
$\frac{7}{2}^-[743]$ (g.s. band)	$\frac{9}{2}^-$	$(7.4\ \pm 0.7)10^4$	$(4.0)10^4$	$(4.2)10^4$
	$\frac{11}{2}^-$	$(1.18\pm 0.16)10^4$	$(1.17)10^4$	$(1.1)10^4$
$\frac{5}{2}^-[752]$	$\frac{5}{2}^-$	$(2.1\ \pm 0.3)10^2$	$(3.2)10^3$	$(5.5)10^2$
	$\frac{7}{2}^-$	$(\sim 2.3)10^2$	$(2.9)10^3$	$(5.4)10^2$
	$\frac{9}{2}^-$	$(1.3\ \pm 0.4)10^2$	$(5.6)10^3$	$(3.5)10^2$
	$\frac{11}{2}^-$	$(\sim 0.46)10^2$	2.1	$(1.2)10^2$
$\frac{9}{2}^-[734]$	$\frac{9}{2}^-$	$(1.9\ \pm 0.3)10^2$	$(4.2)10^3$	$(5.9)10^3$
	$\frac{11}{2}^-$	$(1.7\ \pm 0.4)10^2$	$(2.0)10^2$	$(2.7)10^2$
$\frac{3}{2}^-(\frac{7}{2}[743]*2_\gamma^+)$	$\frac{3}{2}^-$	$(1.3^{+0.4}_{-0.2})10^2$	$(0.8)10^{-2}$	$(0.1)10^{-2}$
or	$\frac{5}{2}^-$	$(0.5\ \pm 0.2)10^2$	0.17	$(0.1)10^{-1}$
$\frac{3}{2}^-[501]$?	$\frac{7}{2}^-$	$(\sim 0.2)\,10^2$	0.19	0.22

ambiguous to use when one deals with two-body operators other than the Hamiltonian for which it has been built. This is the case for the square of the particle total angular momentum $\vec{j}^2$—see, e.g., a discussion of this point in Ref. 42. This is also the case whenever a pairing residual interaction has to be considered, as pointed out within the rotor plus qp framework in Ref. 43. Another deficiency of the whole approach is due to our one qp description of odd nuclei wave functions. Projecting them on good particle number states before Coriolis mixing or evaluating them through a blocking approximation procedure (leading thus to orthonormalization problems for the BCS cores) would not be an easy numerical task and we have therefore preferred at this point to provide an estimate of theoretical "error bars" associated with it, by evaluating as much as possible spectroscopic properties from calculations using *both* adjacent even cores. In this respect the present calculations also constitute only a limited attempt which will need to be (and will be) improved in the near future.

As they now stand, however, our calculations have clearly demonstrated the relevance of the deformed mean fields stemming from HF plus BCS calculations using the Skyrme SIII effective force. As was the case for extreme deformations ($\beta \sim 0.6$) as in fission isomers,[10] or to a lesser extent for weak deformations as in transitional nuclei,[4,9,44] we have shown here that our approach is able to reproduce well low excitation energy spectroscopic properties of deformed nuclei. There are well defined exceptions to this: states which are known to be of a coupled vibration-qp character. As expected, we have not found them in general, thus confirming their "experimental" characterization, tion, moreover, in cases where a doubt was possible the evaluation of some transition probabilities has allowed us to draw unambiguous conclusions. It should be noted incidentally that we have given here *complete* theoretical spectra and not only those states which might have an experimental counterpart.

In view of the success we have met in reproducing both odd-neutron and odd-proton nuclear spec-

TABLE XIV. Comparison of experimental (Refs. 15, 39) and calculated relative $B(M1)$ reduced transition probabilities in ^{235}U. Absolute theoretical $B(M1)$ values are also given (in $\mu_N{}^2$).

	Experimental (relative)	^{234}U+1 qp (relative)	^{236}U+1 qp (relative)	^{234}U+1 qp (absolute)	^{236}U+1 qp (absolute)
$\frac{5}{2}[752]\rightarrow\frac{7}{2}[743]$					
$\frac{7}{2}\rightarrow\frac{7}{2}$	0.27 ± 0.04	0.20	0.27	0.10	0.25
$\frac{7}{2}\rightarrow\frac{9}{2}$	1.0	1.0	1.0	0.52	0.94
$\frac{9}{2}\rightarrow\frac{7}{2}$	<0.1	0.11	10^{-3}	0.048	0.000 78
$\frac{9}{2}\rightarrow\frac{9}{2}$	0.32 ± 0.11	0.23	0.64	0.10	0.43
$\frac{9}{2}\rightarrow\frac{11}{2}$	1.0	1.0	1.0	0.44	0.68
$\frac{11}{2}\rightarrow\frac{9}{2}$	<0.2	0.21	0.015	0.089	0.0070
$\frac{11}{2}\rightarrow\frac{11}{2}$	~0.3	0.22	1.25	0.092	0.56
$\frac{11}{2}\rightarrow\frac{13}{2}$	1.0	1.0	1.0	0.42	0.44
$\frac{9}{2}[734]\rightarrow\frac{7}{2}[743]$					
$\frac{9}{2}\rightarrow\frac{7}{2}$	1.0	1.0	1.0	1.03	0.88
$\frac{9}{2}\rightarrow\frac{9}{2}$	0.48 ± 0.09	0.23	0.10	0.24	0.092
$\frac{9}{2}\rightarrow\frac{11}{2}$	~0.3	0.018	0.13	0.019	0.12
$\frac{11}{2}\rightarrow\frac{9}{2}$	1.0	1.0	1.0	0.76	0.66
$\frac{11}{2}\rightarrow\frac{11}{2}$	0.62 ± 0.13	0.35	0.07	0.27	0.051
$\frac{11}{2}\rightarrow\frac{13}{2}$	<0.2	0.07	0.39	0.056	0.26
$\frac{13}{2}\rightarrow\frac{11}{2}$	1.0	1.0	1.0	0.47	0.60
$\frac{13}{2}\rightarrow\frac{13}{2}$	$0.8\ \pm0.3$	0.82	0.048	0.38	0.029

troscopic properties, and in spite of obvious limitations in its present stage, we think that our approach already has a reasonable predictive power and may provide some guidance for the spectroscopic study of poorly documented nuclear species.

ACKNOWLEDGMENTS

We gratefully acknowledge enlightening discussions with E. Osnes and P. Ring. We have also benefitted from many valuable comments of H. G. Börner, C. Briançon, J. Bettencourt, and A. Gizon whom we want also to thank for having communicated some experimental results prior to publication.

APPENDIX A: $E2,M1$ MOMENTS AND REDUCED TRANSITION PROBABILITIES

For an electromagnetic operator O_μ^λ, the reduced transition probability from a state $|I_1M_1\rangle$ to a state $|I_2M_2\rangle$ is defined by:

$$B(0^\lambda;I_1\rightarrow I_2)=\sum_{\mu M_2}|\langle I_2M_2|0_\mu^\lambda|I_1M_1\rangle|^2$$

and the corresponding electromagnetic moment by

$$\mathscr{M}(0^\lambda,I)=\langle II|0_0^\lambda|II\rangle\ ,$$

where the multipole operators 0_μ^λ are composed of a collective (core) part and of an intrinsic part.

In what follows we will restrict our study to the electric quadrupole ($E2$) and the magnetic dipole

TABLE XV. Dependence of magnetic properties in ^{230}Th+1 qp and ^{236}U+1 qp calculations with respect to the value of g_R and g_s in use. Magnetic moments are expressed in μ_N and $B(M1)$ reduced transition probabilities in $\mu_N{}^2$.

	Usual assignment	Core	$g_R=Z/A$ $g_s^{\rm free}$	$g_R=Z/A$ 0.6 $g_s^{\rm free}$	$g_R^{\rm cranking}$ $g_s^{\rm free}$	$g_R^{\rm cranking}$ 0.6 $g_s^{\rm free}$
$\mu_{5/2^+}$in ^{229}Th	$\frac{5}{2}[633]$	^{230}Th	1.03	0.71	0.94	0.62
$\mu_{3/2^-}$in ^{231}Pa	$\frac{1}{2}[530]$	^{230}Th	3.22	2.24	3.15	0.86
$B(M1;\frac{7}{2}^+\to\frac{5}{2}^+)$	intraband					
in ^{231}Pa	$\frac{5}{2}[633]$	^{230}Th	$(0.26)10^{-2}$	$(0.92)10^{-2}$	$(0.01)10^{-2}$	$(0.12)10^{-2}$
$B(M1;\frac{9}{2}^+\to\frac{7}{2}^+)$	intraband					
in ^{231}Pa	$\frac{5}{2}[633]$	^{230}Th	$(0.38)10^{-2}$	$(1.30)10^{-2}$	$(0.01)10^{-2}$	$(0.17)10^{-2}$
$\mu_{5/2^+}$in ^{237}Np	$\frac{5}{2}[642]$	^{236}U	5.51	4.59	1.71	1.31
$\mu_{5/2^-}$in ^{237}Np	$\frac{5}{2}[523]$	^{236}U	0.83	1.45	0.74	2.21
$\mu_{7/2^-}$in ^{235}U	$\frac{7}{2}[743]$	^{236}U	1.26	−0.57	−1.08	−0.61
$B(M1;\frac{9}{2}^-\to\frac{7}{2}^-)$	interband					
in ^{235}U	$\frac{9}{2}[734]\to\frac{7}{2}[743]$	^{236}U	1.18	0.88	0.69	0.46
$B(M1;\frac{9}{2}^-\to\frac{9}{2}^-)$	interband					
in ^{235}U	$\frac{9}{2}[734]\to\frac{7}{2}[743]$	^{236}U	0.122	0.092	0.070	0.048
$B(M1;\frac{9}{2}^-\to\frac{11}{2}^-)$	interband					
in ^{235}U	$\frac{9}{2}[734]\to\frac{7}{2}[743]$	^{236}U	0.156	0.116	0.091	0.062

$(M1)$ operators. The former is defined by

$$O_\mu^2(\text{core})=e\langle r^2Y_\mu{}^2\rangle_{\text{core}}\ ,$$

$$O_\mu^2(\text{intrinsic})=\sum_{i=1}^{A} er_i{}^2Y_\mu{}^2(\hat{r}_i)\ ,$$

where e is the proton charge and $\langle r^2Y_\mu^2\rangle_{\text{core}}$ is the expectation value for the proton core distribution of the one body operator $r^2Y_\mu^2$.

The $M1$ operator O_μ^1 now is defined by

$$O_\mu^1(\text{core})=\left[\frac{3}{4\pi}\right]^{1/2}\frac{e\hbar}{2Mc}g_RR_\mu\ ,$$

$$O_\mu^1(\text{intrinsic})=\left[\frac{3}{4\pi}\right]^{1/2}\frac{e\hbar}{2Mc}(g_ss_\mu+g_ll_\mu)\ ,$$

where M is the average nucleonic mass, g_R, g_s, and g_l are the core, spin, and orbital gyromagnetic ratios, and R_μ, s_μ, and l_μ are the μ components of the core, intrinsic spin, and orbital angular momenta.

One may rewrite the total $M1$ operator

$$O_\mu^1=\left[\frac{3}{4\pi}\right]^{1/2}\frac{e\hbar}{2Mc}(g_RI_\mu+G_\mu^1)\ ,$$

where

$$G_\mu^1=(g_l-g_R)l_\mu+(g_s-g_R)s_\mu\ .$$

Each eigenstate $|\gamma IM\rangle$ of the Hamiltonian H is expressed through Eq. (5) in terms of standard unified model basis states[3]:

$$\langle\theta_i\,|\,\alpha IMK\rangle=\left[\frac{2I+1}{16\pi^2}\right]^{1/2}\times[D_{MK}^I(\theta_i)\,|\,\alpha K\rangle+(-)^{I+K}D_{M-K}^I(\theta_i)\,|\,\overline{\alpha K}\rangle]\ .$$

To evaluate moments and reduced transition probabilities associated with a multipole operator O_μ^λ we must compute $\langle\gamma_2I_2M_2\,|\,O_\mu^\lambda\,|\,\gamma_1I_1M_1\rangle$ matrix elements, and thence in the qp basis

$\langle \alpha_2 I_2 M_2 K_2 | O_\mu^\lambda | \alpha_1 I_1 M_1 K_1 \rangle$ matrix elements.

Practically, apart from the I_μ term in the O_μ^1 operator defined above which is easily handled in the laboratory frame, the remaining part of O_μ^1, as well as the full O_μ^2 operator, being defined in terms of sp wave functions, should be transformed into the intrinsic frame. Transforming the tensors O_μ^λ into the latter and using well known rotation matrix properties, one gets finally for the O_μ^λ matrix elements:

$$\begin{aligned}
\langle \alpha_2 I_2 M_2 K_2 | O_\mu^\lambda | \alpha_1 I_1 M_1 K_1 \rangle
&= \frac{(2I_1+1)^{1/2}(2I_2+1)^{1/2}}{2}(-)^{M_2-K_2}\begin{bmatrix} I_2 & \lambda & I_1 \\ -M_2 & \mu & M_1 \end{bmatrix} \\
&\quad\times\sum_\nu \left\{ \begin{bmatrix} I_2 & \lambda & I_1 \\ -K_2 & \nu & K_1 \end{bmatrix} [\langle \alpha_2 K_2 | O_\nu^\lambda | \alpha_1 K_1 \rangle + (-)^{K_1-K_2+\lambda}\langle \overline{\alpha_2 K_2} | O_{-\nu}^\lambda | \overline{\alpha_1 K_1} \rangle] \right. \\
&\quad\left. +(-)^{I_1+K_1}\begin{bmatrix} I_2 & \lambda & I_1 \\ -K_2 & \nu & -K_1 \end{bmatrix} [\langle \alpha_2 K_2 | O_\nu^\lambda | \overline{\alpha_1 K_1} \rangle + (-)^{K_1-K_2+\lambda}\langle \overline{\alpha_2 K_2} | O_{-\nu}^\lambda | \alpha_1 K_1 \rangle] \right\} .
\end{aligned}$$

Now using the time-reversal properties of $|\alpha K\rangle$ states and O_ν^λ operators, namely

$$|\overline{\alpha K}\rangle = \mathscr{C}|\alpha K\rangle,\ \mathscr{C}|\overline{\alpha K}\rangle = (-)^{2K}|\alpha K\rangle$$

and

$$\mathscr{C} O_\nu^\lambda \mathscr{C}^+ = c_\lambda (-)^{\lambda+\nu} O_{-\nu}^\lambda$$

[with $c_\lambda = (-)^\lambda$ for $E\lambda$ operators and $c_\lambda = (-)^{\lambda+1}$ for $M\lambda$ operators], one may rewrite in a more compact form these matrix elements.

A. $B(E2)$ reduced transition probabilities

$$B(E2;\gamma_1 I_1 \to \gamma_2 I_2) = \left[\sum_{M_1 M_2} F(\gamma_1 I_1 M_1, \gamma_2 I_2 M_2) + O_0^2(\text{core}) \sum_{\alpha K} C_{\alpha K}^{\gamma_1} C_{\alpha K}^{\gamma_2} \sqrt{2I_2+1}(-)^{I_1+K}\begin{bmatrix} I_1 & 2 & I_2 \\ K & 0 & -K \end{bmatrix} \right]^2 ,$$

where O_0^2 (core) defined above is given in terms of the HF plus BCS core charge quadrupole moment Q_0 calculated in I as

$$O_0^2(\text{core}) = eQ_0 \left[\frac{5}{16\pi} \right]^{1/2} .$$

In the preceding the quantity F is defined as

$$\begin{aligned}
F(\gamma_1 I_1 M_1, \gamma_2 I_2 M_2) &= (2I_1+1)^{1/2}(2I_2+1)^{1/2}\begin{bmatrix} I_2 & 2 & I_1 \\ -M_2 & M_2-M_1 & M_1 \end{bmatrix}(-)^{M_2-I_2} \\
&\quad\times\left\{ \sum_{\alpha_1 K_1 \alpha_2 K_2} C_{\alpha_1 K_1}^{\gamma_1} C_{\alpha_2 K_2}^{\gamma_2} (u_{\alpha_1 K_1} u_{\alpha_2 K_2} - v_{\alpha_1 K_1} v_{\alpha_2 K_2}) \right.
\end{aligned}$$

$$\times\Bigg[(-)^{I_2-K_2}\begin{pmatrix} I_2 & 2 & I_1\\ -K_2 & K_2-K_1 & K_1\end{pmatrix}\langle\alpha_2K_2\,|\,O_{K_2-K_1}^{2}(\text{intrinsic})\,|\,\alpha_1K_1\rangle$$

$$+\begin{pmatrix} I_2 & 2 & I_1\\ -K_2 & 2 & -K_1\end{pmatrix}\delta_{K_1+K_2,2}\langle\alpha_2K_2\,|\,O_2^2(\text{intrinsic})\,|\,\overline{\alpha_1K_1}\rangle$$

$$-\begin{pmatrix} I_2 & 2 & I_1\\ -K_2 & 1 & -K_1\end{pmatrix}\delta_{K_1,K_2}\delta_{K_1,1/2}\langle\alpha_2K_2\,|\,O_1^2(\text{intrinsic})\,|\,\overline{\alpha_1K_1}\rangle\Bigg]\Bigg\}\,,$$

where u and v are the usual pairing occupation factors, C_{IK}^{γ} are the Coriolis mixing factors of Eq. (5), and $|\alpha K\rangle$ and $|\overline{\alpha K}\rangle$ are the sp wave functions of the HF state defined by the quantum number set (αK) and its time-reversal conjugate.

B. $B(M1)$ reduced transition probabilities

$$B(M1;\gamma_1 I_1\rightarrow\gamma_2 I_2)=\frac{3}{4\pi}\mu_N{}^2\sum_{M_1M_2}\left(A_{M_1M_2}^{\gamma_1I_1,\gamma_2I_2}+B_{M_1M_2}^{\gamma_1I_1,\gamma_2I_2}\right)^2\,,$$

where μ_N is the nuclear magneton and the quantities A and B are defined as follows:

$$A_{M_1M_2}^{\gamma_1I_1,\gamma_2I_2}=(2I_1+1)^{1/2}(2I_2+1)^{1/2}\begin{pmatrix} I_2 & 1 & I_1\\ -M_2 & M_2-M_1 & M_1\end{pmatrix}$$

$$\times\Bigg\{\sum_{\alpha_2K_2}C_{\alpha_2K_2}^{\gamma_2}(-)^{M_2-K_2}\sum_{\alpha_1K_1}C_{\alpha_1K_1}^{\gamma_1}\Bigg[\begin{pmatrix} I_2 & 1 & I_1\\ -K_2 & K_2-K_1 & K_1\end{pmatrix}\langle\alpha_2K_2\,|\,G_{K_2-K_1}^{1}\,|\,\alpha_1K_1\rangle$$

$$+\,\delta_{K_1,K_2}\delta_{K_1,1/2}(-)^{K_2+I_2}\begin{pmatrix} I_2 & 1 & I_1\\ -\frac{1}{2} & 1 & -\frac{1}{2}\end{pmatrix}\langle\alpha_2K_2\,|\,G_1^1\,|\,\overline{\alpha_1K_1}\rangle\Bigg]\Bigg\}\,,$$

and

$$B_{M_1M_2}^{\gamma_1I_1,\gamma_2I_2}=g_R\delta_{I_1,I_2}\left[\sum_{\alpha K}C_{\alpha K}^{\gamma_1}C_{\alpha K}^{\gamma_2}\right]$$

$$\times\left\{\delta_{M_1,M_2}M_1+\delta_{M_1,M_2+1}\left[\frac{(I_1+M_1)(I_1-M_2)}{2}\right]^{1/2}-\delta_{M_1,M_2-1}\left[\frac{(I_1-M_1)(I_1+M_2)}{2}\right]^{1/2}\right\}.$$

C. Quadrupole moment

Usually, the quadrupole moment Q of a nuclear state having a total spin I is defined in terms of the quantity $\mathcal{M}(E2,I)$ by:

$$Q^I=\left[\frac{16\pi}{5}\right]^{1/2}\frac{\mathcal{M}(E2,I)}{e}\,.$$

For a Coriolis mixed state $|\gamma I\rangle$ one then obtains for the quadrupole moment

$$Q^{\gamma I}=\left[\frac{16\pi}{5}\right]^{1/2}F(\gamma II,\gamma II)$$

$$+Q_0\sum_{\alpha K}\left[(C_{\alpha K}^{\gamma})^2\frac{3K^2-I(I+1)}{(I+1)(2I+3)}\right]\,.$$

D. Magnetic moment

The usual definition of the magnetic moment of a nuclear state having a total spin I, in terms of the quantity $\mathscr{M}(M1,I)$ is

$$\mu^I = \left[\frac{4\pi}{3}\right]^{1/2} \mathscr{M}(M1,I) .$$

For a Coriolis state $|\gamma I\rangle$ one then obtains for the magnetic moment

$$\mu^{\gamma I} = \mu_N (A_{II}^{\gamma I,\gamma I} + B_{II}^{\gamma I,\gamma I}) .$$

APPENDIX B: NUMERICAL CALCULATION OF INTRINSIC $E2$ AND $M1$ MATRIX ELEMENTS

In this appendix, we will give some details on the calculation of matrix elements of one-body operators O between Hartree-Fock states $|\alpha K\rangle$. Since we are concerned with $E2$ and $M1$ electromagnetic properties, the operators O to be considered are s_z, $s_\pm$, x, y, z, ∂_x, ∂_y, ∂_z, and some combinations of the latter. Hartree-Fock states are expanded on axially symmetrical harmonic oscillator basis states $|n_z n_\perp \Lambda \Sigma\rangle$. For such states, which are eigenstates of the $\vec{s}^{\,2}$ and s_z operators, the matrix elements of the spin operators are trivial. The computation of matrix elements in the $|n_z n_\perp \Lambda\rangle$ basis of operators acting only on space variables is greatly facilitated by noting that upon making a canonical transformation on b_x^+, $b_y^+ (b_x, b_y)$ creation (annihilation) operators, one may view such basis states as eigenstates of new quanta number operators $n_\alpha = b_\alpha^+ b_\alpha$ and $n_\beta = b_\beta^+ b_\beta$ given[45] by

$$b_\alpha^+ = \frac{1}{\sqrt{2}}(b_x + i b_y) ,$$

$$b_\beta^+ = \frac{1}{\sqrt{2}}(b_x - i b_y) , \tag{B1}$$

in terms of the corresponding quantum number n_α and n_β, the basis state $|n_z n_\perp \Lambda\rangle$ may be written

$$|n_z n_\perp \Lambda\rangle \equiv |n_z n_\alpha n_\beta\rangle$$

$$= (-)^\beta \frac{(b_z^+)^{n_z}}{\sqrt{n_z!}} \frac{(b_\alpha^+)^{n_\alpha}}{\sqrt{n_\alpha!}} \frac{(b_\beta^+)^{n_\beta}}{\sqrt{n_\beta!}} |000\rangle , \tag{B2}$$

where $|000\rangle$ is the vacuum and with

$$n_\alpha = (n_\perp + \Lambda)/2 ,$$

$$n_\beta = (n_\perp - \Lambda)/2 . \tag{B3}$$

From usual relations between b_i^+, b_i and x_i, ∂_{x_i} operators as

$$z = \frac{1}{\sqrt{2}c_z}(b_z^+ + b_z) ,$$

$$\partial_z = -\frac{c_z}{\sqrt{2}}(b_z^+ - b_z) , \tag{B4}$$

where c_z is the inverse of the harmonic oscillator length $(c_z = \sqrt{m\omega_z/\hbar})$, one gets using Eq. (B2)

$$x = \frac{1}{2c_\perp}(b_\alpha^+ + b_\beta^+ + b_\alpha + b_\beta) ,$$

$$y = \frac{i}{2c_\perp}(-b_\alpha^{+b_\beta^+} + b_\alpha - b_\beta) ,$$

$$\partial_x = \frac{c_\perp}{2}(-b_\alpha^+ - b_\beta^+ + b_\alpha + b_\beta) , \tag{B5}$$

$$\partial_y = \frac{i c_\perp}{2}(b_\alpha^+ - b_\beta^+ + b_\alpha - b_\beta) ,$$

(with $c_\perp = \sqrt{m\omega_\perp/\hbar}$).

For $M1$ properties one needs, apart from spin operator matrix elements, the matrix elements of the l_+, l_-, and l_z operators. The latter are easily expressed in terms of b, b^+ operators from Eqs. (B4) and (B5).

For $E2$ properties, one has to take into account the $r^2 Y_\mu^2$ operators whose expressions in terms of x, y, and z are well known, and which are thus easily calculated through Eqs. (B4) and (B5).

[1]J. Libert and P. Quentin, Phys. Rev. C 25, 571 (1982).

[2]M. Beiner, H. Flocard, Nguyen Van Giai, and P. Quentin, Nucl. Phys. A238, 29 (1975).

[3]See, e.g., Å. Bohr and B. Mottelson, *Nuclear Structure* (Benjamin, New York, 1975), Vol. II.

[4]M. Meyer, J. Danière, J. Letessier, and P. Quentin, Nucl. Phys. A316, 93 (1979).

[5]M. A. Deleplanque, C. Gerschel, N. Perrin, and P. Quentin, Phys. Lett. 46B, 317 (1973).

[6]N. de Takacsy and S. Das Gupta, Nucl. Phys. A263, 237 (1976); S. Das Gupta and N. de Takacsy, Am. J. Phys. 44, 47 (1976).

[7]D. W. L. Sprung, S. G. Lie, M. Vallières, and P. Quentin, Nucl. Phys. A326, 37 (1979).

[8]M. J. Giannoni and P. Quentin, Phys. Rev. C 21, 2076 (1980).

[9]J. Tréherne, J. Genevey, R. Béraud, A. Charvet, R. Duffait, M. Meyer, F. Beck, and T. Byrski, Nucl. Phys. A342, 357 (1980).

[10]J. Libert, M. Meyer, and P. Quentin, Phys. Lett. 95B, 175 (1980).

[11]T. Yamazaki, in *Mesons in Nuclei,* edited by M. Rho and D. Wilkinson (North-Holland, Amsterdam, 1978), Vol. II, p. 651; A. Arima and H. Hyuga, *ibid.*, p. 683.

[12]S. G. Nilsson and O. Prior, K. Dan. Vidensk. Selsk. Mat. Fys. Medd. 32, No. 16 (1960).

[13]O. Prior, F. Boehm, and S. G. Nilsson, Nucl. Phys. A110, 257 (1968).

[14]For the sake of comparison with the results of our calculations, we will use experimental energy spectra taken from the compilation of Ref. 15 ($A = 231, 235, 239$); and Ref. 16 ($A = 229, 233, 237, 241$) as well as from the review article of Chasman *et al.* (Ref. 17). These references summarize all available data up to 1977–1978. More recent data will be quoted when necessary.

[15]M. Schmerck, Nucl. Data Sheets 21, 91 (1977); 21, 117 (1977); 21, 153 (1977).

[16]K. S. Toth, Nucl. Data Sheets 24, 263 (1978); Y. A. Ellis, *ibid.* 24, 289 (1978); 23, 71 (1978); 23, 123 (1978).

[17]R. R. Chasman, I. Ahmad, A. M. Friedman, and J. R. Erskine, Rev. Mod. Phys. 49, 833 (1977).

[18]Y. A. Ellis, J. F. Emery, and K. S. Toth, Phys. Rev. C 20, 799 (1979).

[19]J. Almeida, T. v. Egidy, P. H. M. Van Assche, H. G. Börner, W. F. Davidson, K. Schreckenbach, and A. I. Namenson, Nucl. Phys. A315, 71 (1979).

[20]J. de Bettencourt, C. Briançon, A. Gizon, J. Libert, J. P. Thibaud, and R. J. Walen (unpublished); J. de Bettencourt (private communication).

[21]M. W. Johnson, R. C. Thompson, and J. R. Huizenga, Phys. Rev. C 17, 934 (1978).

[22]H. G. Börner, H. R. Koch, H. Seyfarth, T. v. Egidy, W. Mampe, J. A. Pinston, K. Schreckenbach, and D. Heck, Z. Phys. A 286, 31 (1978).

[23]T. v. Egidy, J. Almeida, G. Barreau, H. G. Börner, W. F. Davidson, R. W. Hoff, P. Jeuch, K. Schreckenbach, D. D. Warner, and D. H. White, Phys. Lett. 81B, 281 (1979).

[24]R. R. Chasman, Phys. Rev. C 14, 1935 (1976).

[25]R. D. Griffioen, R. C. Thompson, and J. R. Huizenga, Phys. Rev. C 18, 671 (1978).

[26]L. Gonzalez, R. Gaeta, E. Vaño, and J. M. Los Arcos, Nucl. Phys. A324, 126 (1979).

[27]D. H. White, G. Barreau, H. G. Börner, W. F. Davidson, R. W. Hoff, P. Jeuch, W. Kane, K. Schreckenbach, T. v. Egidy, and D. D. Warner, in *Neutron Capture Gamma-Ray Spectroscopy,* edited by R. E. Chrien and W. R. Kane (Plenum, New York, 1979), p. 801; H. G. Börner (private communication).

[28]T. Grotdal, J. Limstrand, K. Nybö, K. Skak, and F. T. Thorsteinsen, Nucl. Phys. A189, 592 (1972).

[29]P. Quentin, in *Nuclear Self-Consistent Fields,* edited by G. Ripka and M. Porneuf (North-Holland, Amsterdam, 1975), p. 297.

[30]P. Jeuch, T. v. Egidy, K. Schreckenbach, W. Mampe, H. G. Börner, W. F. Davidson, J. A. Pinston, R. Roussille, R. C. Greenwood, and R. E. Chrien, Nucl. Phys. A317, 363 (1979).

[31]*Table of Isotopes,* 7th ed., edited by C. M. Lederer and V. S. Shirley (Wiley, New York, 1978).

[32]L. A. Kroger and C. W. Reich, Nucl. Phys. A259, 29 (1976).

[33]H. Ton, S. Roodbergen, J. Brasz, and J. Blok, Nucl. Phys. A155, 245 (1970).

[34]P. Hornshöj, P. Tidemand-Petersson, R. Kaczarowski, B. Kotlinska, and J. Zylicz, Nucl. Phys. A248, 406 (1975).

[35]J. O. Newton, Nucl. Phys. 5, 218 (1958).

[36]J. O. Newton, Nucl. Phys. 3, 345 (1957).

[37]S. W. Yates, I. Ahmad, A. M. Friedman, F. J. Lynch, and R. E. Holland, Phys. Rev. C 11, 599 (1975).

[38]S. B. Patel, A. P. Agnihotry, P. N. Tandon, and K. P. Gopinathan, Phys. Rev. C 9, 1515 (1974).

[39]F. S. Stephens, M. D. Holtz, R. M. Diamond, and J. O. Newton, Nucl. Phys. A115, 129 (1968).

[40]Å. Bohr, K. Dan. Vidensk. Selsk. Mat Fys. Medd. 26, No. 14 (1952); A. K. Kerman, *ibid.* 30, No. 15 (1956); J. R. Erskine and W. W. Buchner, Phys. Rev. 133, B370 (1964); W. Scholz and F. B. Malik, *ibid.* 176, 1355 (1968) and references quoted therein; M. E. Bunker and C. W. Reich, Rev. Mod. Phys. 43, 348 (1971); W. Ogle, S. Wahlborn, R. Piepenbring, and S. Fredriksson, *ibid.* 43, 424 (1971); B. S. Nielssen and M. E. Bunker, Nucl. Phys. A245, 376 (1975); E. Osnes, J. Rekstad, and O. K. Gjötterud, *ibid.* A253, 45 (1975); J. Rekstad, *ibid.* A247, 7 (1975); B. H. Haas and P. Taras, Can. J. Phys. 52, 49 (1974); D. D. Warner, Ph.D. thesis, University of Sussex, 1975 (unpublished); R. Popli, F. A. Rickey, and P. C. Simms, Phys. Rev. C 22, 1121 (1980); R. Popli, J. A. Grau, S. I. Popik, L. E. Samuelson, F. A. Rickey, and P. C. Simms, *ibid.* 20, 1350 (1979).

[41]J. Libert and P. Quentin, Institut Laue-Langevin, (ILL) Grenoble Report SP81-53, 1981.

[42]P. Ring (private communication); see, however, K. Neergård, Phys. Lett. 89B, 5 (1979).

[43]T. Engeland and J. Rekstad, Phys. Lett. 89B, 8 (1979); J. Rekstad and T. Engeland, Phys. Lett. 89B, 316 (1980).

[44]P. Quentin, M. Meyer, J. Letessier, J. Libert, and M. G. Desthuilliers-Porquet, in *Nuclear Spectroscopy of Fission Products,* edited by T. V. Egidy (Institute of Physics, Bristol, 1980), p. 280; M. G. Desthuilliers-Porquet, J. Sauvage-Letessier, M. Meyer, and P. Quentin (unpublished).

[45]P. Quentin and R. Babinet, Nucl. Phys. A156, 365 (1970).